



Liquid Metal Cooled Nuclear Power Plants: A Brief Review

Seth Kofi Debrah^{1, 3*}, Ethna Norkplim Afua Adzokpa¹, Kwasi Oppong Kyekyeku¹, Edward Shitsi^{1,2}, Emmanuel Maurice Arthur^{1,3}

¹Department of Nuclear Engineering, School of Nuclear and Allied Sciences, University of Ghana. P.O. Box AE1, Kwabenya, Accra

²Nuclear Research Centre, National Nuclear Research Institute, Ghana Atomic Energy Commission. P.O. Box LG 80, Legon, Accra

³Nuclear Power Institute, Ghana Atomic Energy Commission. P.O. Box LG 80, Legon, Accra

*Correspondence to: Seth Kofi Debrah, Ethna Norkplim Afua Adzokpa, Kwasi Oppong Kyekyeku, Edward Shitsi, Emmanuel Maurice Arthur, Department of Nuclear Engineering, School of Nuclear and Allied Sciences, University of Ghana. P.O. Box AE1, Kwabenya, Accra, Tel no: 233243215604; E-mail: s.kdebrah@gaecgh.org

Received date: Sep 01, 2021; Accepted date: November 19, 2021; Published date: November 29, 2021

Citation: Debrah s k, Adzokpa N A, Kyekyeku K O, Shitsi E, Maurice Arthur. Liquid Metal Cooled Nuclear Power Plants: A Brief Review. J Nucl Ene SciPower Generat Techno.10(11).

Abstract

Liquid metal cooled nuclear reactors for power generation are receiving new research interest because of competitive design technology compared to that of Light Water Reactors (LWRs). And also, out of six GEN IV reactor technologies to be designed and operated in the near future, two are liquid metal cooled reactors, namely Sodium Cooled Fast Reactors (SFRs) and Lead Cooled Fast reactors (LFRs). It is therefore important to carry out various studies related to liquid metal cooled nuclear reactors to support safe design and operation of SFRs and LFRs in the near future. This study carried out brief review on sodium, lead, and lead-bismuth-eutectic liquid metal cooled fast reactors. The review also covers recent experimental and computational studies as well provided some research concerns of liquid metal cooled NPPs that need attention to further contribute to the efforts being made to design and operate liquid metal cooled NPPs for electricity generation.

Introduction

Research activities towards the development of liquid metal cooled fast reactor (LMFR) concepts, design and operation aim at addressing safety concerns of these reactor systems prior to their commercialization. These research activities include studies related to thermal-hydraulics, neutronics, corrosion and erosion of structural materials, seismic risk, in-service inspection of core, refueling at high temperature, spent fuel management, chemistry control, prevention of flow blockage, radiation damage development of measuring devices, and advanced Modeling & Simulation (M&S) tools among others.

When comparing nuclear technologies in an attempt to select one technology over the other, the parameters such as safety risk, fuel cycle, economics, experience base and proliferation among others are considered. The safety risk consideration takes into account among other safety concerns the safety of the design in terms of passive safety or inherent safety as well as Probabilistic Safety Assessment

(PSA) results such as Lower core damage frequency when compared with existing operating Light Water Reactors (LWRs) as having medium risk of design and operation. Fuel cycle consideration takes into account the volume/amount of nuclear waste produced. The fuel cycle option takes into consideration the possibility of recycling or reprocessing of the nuclear waste generated and as a result reducing the volume of the nuclear waste generated. The possibility of making use of the plutonium produced in the nuclear waste is highly taken into consideration in the case of LMFRs. Economics consideration takes into account the reactor size with its corresponding cost of construction. Economics rating consideration does not take into account the cost of refueling, operation and maintenance. Experiencing base consideration takes into account the history of operation of the reactor or Nuclear Power Plant (NPP), weather the plant has been in operation or not since new NPP technologies might not have any history of operation. Proliferation consideration takes into account how the separated plutonium from reprocessing of nuclear waste is used peacefully and does not fall into the wrong hands. GEN IV reactors were selected based on factors such as safety, sustainability, economics, physical security, proliferation resistance, and waste minimization. Economics takes into consideration total cost of constructing a particular advanced nuclear reactor technology for power generation. The cost estimation also takes into consideration factors such as Size, Safety, Security and Weapons Proliferation Risk, Versatility, Waste Management, and Environmental Effects. These advanced GEN IV reactor technologies include Gas-Cooled Fast Reactor, Lead-Cooled Fast Reactor, Molten Salt Reactor, Sodium-Cooled Fast Reactor, Supercritical Water-Cooled Reactor, and Very High Temperature Reactor (Arostegui and Holt, 2019). Thus, research activities that aim at addressing safety related issues in the design and operation of LMFRs cannot be over-emphasized. The research activities also help in selecting one NPP technology over others for construction and commercialization.

Among other authors made efforts to put together various studies on LMFRs. Wang 2017 carried out review on Heat eXchanger Tube Rupture (HXTR) accident (or Steam Generator Tube Rupture (SGTR) accident) from 1992 to 2016. His review mainly considered experimental and simulation studies involving HXTR (or SGTR). He found out that issues mostly investigated for experimental study include pressure evolution, vapor transmission, fragmentation behavior, physics of the thermal and hydraulic interactions between heavy liquid metal (HLM) and water; and issues mostly investigated for simulation study include pressure evolution and steam transmission. He mentioned that issues such as propagation of the pressure waves and sloshing of the primary coolant pool (the primary HLM pool could cause some sort of mechanical impact on structures of contact) need more research attention to help further understand these phenomena, and more experimental facilities and numerical tools are needed for these types of studies.

Carried out review on lead cooled fast reactors LFRs pointing out developmental challenges as well as other research concerns that need attention. The review mainly focused on flow and heat transfer characteristics of lead/LBE coolant, and thermal-hydraulic analysis of the reactor core, lead/LBE pool and reactor system. They also mentioned that the choice of a particular LMFR over the other depends on corrosion of the structural material by the liquid metal coolant, the operating temperature limitations with respect to structure integrity of the various materials used for the system design, and

formation of toxic radioactive Po-210 among other factors of consideration to ensure system safety and longer operation lifetime of the reactor. Further studies including developing new experimental methods, integral effect caused by accidents, characteristics of lead/LBE-gas two-phase flow with respect to SGTR and gas-lift pump assessment that need attention were pointed out in this review.

Carried out review on computational modeling methods for thermal stratification phenomenon in SFRs (system-level methods and CFD methods) as well provided further research areas such as employing machine learning methods to increase accuracy of 1-D models (system-level methods), and using reduced order modeling (ROM) to decrease computational time of CFD models, that need attention. They mentioned that the thermal stratification phenomenon might cause neutronic and thermal-hydraulic instabilities in the reactor core, could lead to damages of both the reactor vessel and in-vessel components as a result of thermal fatigue cracking growth, impede natural circulation heat removal during accidents and introduce uncertainties to the core safety of SFRs. Roelofs discussed the state-of-the-art, challenges and the future perspectives of Liquid metal heat transfer, Fluid-Structure interaction, Fuel assembly thermal hydraulics, Coolant solidification, Efficient 3-D system modelling, and Validation of simulation approaches, and provided the following concluding points based on his point of view on the afore-mentioned areas of study .

- Development of an anisotropic turbulence heat flux model with wall functions which can deal with all flow regimes simultaneously.
- Determination of the effect of fuel assembly deformations occurring as a result of operation at elevated temperatures and in an irradiation environment, including surface deformations, e.g. by corrosion or other chemical interactions.
- Determination of the effect of fuel assembly blockages on flow and heat transfer.
- Further development of efficient 3-dimensional numerical tools for system thermal hydraulic simulation,
- Further developments in experimental techniques for liquid metals.
- Increase of the validation base for nuclear liquid metal applications with experimental and high-fidelity simulation data.

This study carried out brief review on sodium, lead and lead-bismuth-eutectic liquid metal cooled fast reactors. The review also covers recent experimental and computational studies as well provided some research gaps of liquid metal cooled NPPs that need attention to further contribute to the efforts being made to design and operate liquid metal cooled NPPs for electricity generation and other non-power applications. The experimental and computational studies are provided in a more educative manner, and turbulence modelling and near-wall treatment which is a challenge when using CFD codes are also provided in a more simplified and educative manner.

Liquid metal cooled fast reactors are the type of fast reactors that use liquid metals such as sodium (Na), lead (Pb), and lead-bismuth eutectic (LBE) (or lead-bismuth alloy) as their coolants and they are classified according to their liquid metal coolants used. This reactor can transform a fertile material into a fissile material such as ^{238}U into ^{239}Pu and ^{232}Th into ^{233}U . The concept of this reactor type is very practicable from the fuel utilization perspective. Also, this type of reactor is exemplified by high power density because they do not have moderators. The high-power density properties require this reactor's cores to be small. The coolant temperature rise in the core for this type of reactors is high and hence results in higher efficiency of electric power generation. The most common liquid metal coolants used in the liquid metal cooled fast reactors are sodium and lead.

Schematics of the sodium-cooled fast reactors (SFRs) and lead-cooled fast reactors (LFRs) is presented (Figures 1, 2, 3) (Arostegui and Holt, 2019). For the sodium-cooled fast reactors, there are two major design types which are the pool and loop types. For the loop design of a sodium-cooled fast reactor, the secondary sodium loop removes heat from the pool design, the secondary sodium loop removes heat from the primary sodium pool inside the reactor vessel whilst for the pool design, the secondary sodium loop removes heat from the primary sodium pool inside the reactor vessel. Similarly, for the lead or lead-bismuth-eutectic pool design, the secondary water loop removes heat from the primary lead or lead-bismuth-eutectic pool inside the reactor vessel.

Few sodium-cooled fast reactors have been developed and run in the range of a medium size (150–500 MWe) to a large size (above 1000 MWe). The sodium-cooled fast reactor core outlet temperatures are usually 530–550°C. The main safety quality with sodium-cooled fast reactor is that the primary system runs at mostly atmospheric pressure, pressurized wholly to the magnitude required to transport the fluid alongside its great heat transfer at the core and a wide gap to coolant boiling (Arostegui and Holt, 2019).

The lead-cooled fast reactors on the other hand have low power density and are **intrinsic circulation** cooled reactors with fissile independent core designs with a longer refueling period. The lead-cooled fast reactors have been developed and run in the range of 50 MWe–150 MWe which is the small battery type of systems to medium size (300–400 MWe), and to a large size (1200 MWe). The advanced lead-cooled fast reactor outlet coolant temperatures vary from 550 to 800°C, relying on the preference and suitability of structural materials and fuels. The wide coolant-temperature span of the lead-cooled fast reactors can be put to use in **hydrogen production** through the thermochemical procedure and for this reason it is more preferable than the sodium-cooled fast reactor (Arostegui and Holt, 2019).

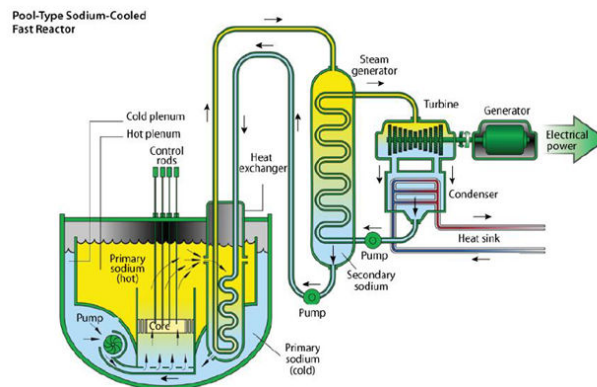


Figure1: Pool type sodium-cooled fast reactor (Arostegui and Holt, 2019)

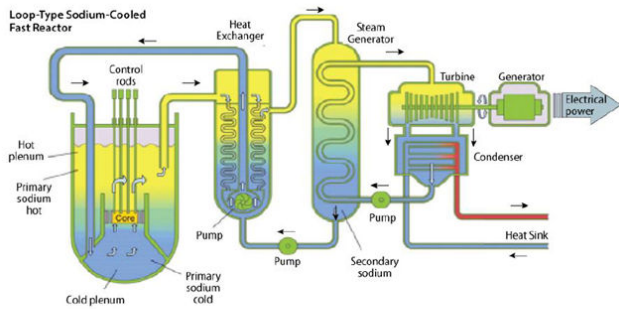


Figure 2. Loop type sodium-cooled fast reactor (Arostegui and Holt, 2019)

5

Figure 2: Loop type sodium-cooled fast reactor (Arostegui and Holt, 2019)

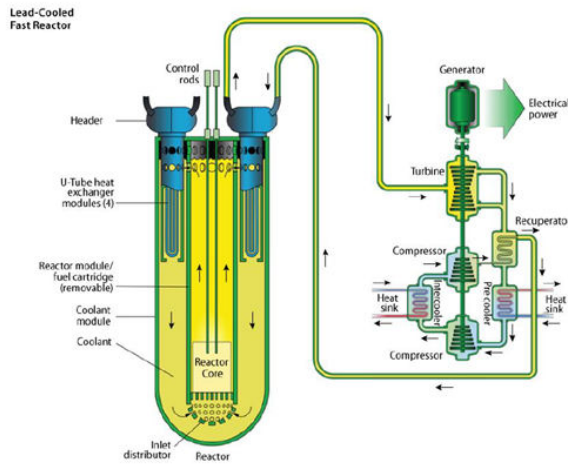


Figure3: Lead Cooled fast reactor (Arostegui and Holt, 2019)

Table 1 shows comparison of LMFRs and LWRs. It can be observed from the table that outlet coolant temperature consideration of reactor systems is important as it directly relates to the thermal efficiency of the reactor system. LMFRs have higher thermal efficiency than that of PWRs and BWRs whereas SCWRs have higher thermal efficiency than that of LMFRs.

Table 1: Comparison of Liquid Metal Cooled Fast Reactors (LMFRs) and Light Water Cooled Reactors (LWRs) (Kadak; Arostegui and Holt, 2019)

	Liquid Metal Cooled Fast Reactors (LMFRs)		Light Water-Cooled Reactors (LWRs)		
	LFR	SFR	PWR	BWR	SCWR
Outlet Temp °C	480-570 °C	500-550	315	285	510-625
Electrical power rating (MW)	20-180; 300-1200;	50-150; 300-1500;	≤1400	500-600; 900-1100; 1400	300-700; 1000-1500

	600-1000	600-1500;			
Thermal efficiency %	41-43	40	33	32-33	45-50
Pressure (MPa)	0.1 MPa	7.8-20 MPa	15 MPa	7 MPa	22-28 MPa

LFR-Lead Cooled Fast Reactor; SFR-Sodium Cooled Fast Reactor; PWR-Pressurized Water Cooled Reactor; BWR-Boiling Water Cooled Reactor; SCWR-Supercritical Water Cooled Reactor. Thermodynamic properties of coolants are temperature dependent and thus vary with temperature. Table 2 shows approximate values of properties of Pb, Na and LBE at 427°C and that of water at 5°C.

Table 2: Properties of Liquid Metal Coolants compared with that of Water (Cheng et al., 2018, Sobolev, 2010)

Properties	Liquid metal coolants at 427°C			Water coolant at 5°C
	Lead	Sodium	LBE	Water
Density, kgm-3	10480	847	10150	1000
Specific Heat, Jkg-1K-1	150	1300	150	4200
Thermal conductivity, wm-1K-1	16	70	13	0.5576
Viscosity (Pa s)	0.00215	0.00027	0.0015	0.001519
Maximum velocity, ms-1	2.5	10	2.5	—
Melting/Freezing point (°C)	328	98	125	0°C
Boiling point (°C)	1750	883	1670	100

Lead-bismuth eutectic (LBE)

Melting and boiling points of liquid metals are also taken into consideration in the design of LMFRs. Table 3 shows melting and boiling points of some liquid metals. Lead, **Lead-bismuth eutectic (LBE)** and Sodium are being considered for the design of advanced LMFRs. From the Table 3, and considering only these three (3) liquid metals, lead has highest melting and boiling points, and sodium has the lowest melting and boiling points.

Table 3: Melting and Boling points of Liquid metal coolants (Cheng et al., 2018, Sobolev, 2010)

Coolant	Melting point (°C)	Boiling point (°C)
Lead	328	1750
Lead-bismuth eutectic (LBE)	125	1670

Sodium	98	883
NaK	-11	785
Mercury	-39	357
Tin	232	2602

Efforts to build and operate LMFRs for power generation has started before 1960, and these efforts have led to the design of LMFRs currently in operation and yet to be built for power generation. Tables 4A-4D show some LMFRs that have been operated and now out of operation, currently in-operation, and yet to be built in the near future (Kadak 2017).

Table 4A : Liquid Metal Cooled Fast Reactors (LMFRs) Out-of-operation

Reactor Name	Country	Power Level (MWe)	Coolant	Year of operation
BN-350 (Aktau NPP)	Kazakhstan	350 FAST	Sodium	1973-1993/8
FERM 1	USA	69 FAST (200 MWt)	Sodium	1963-1972
Superphéni x	France	1200 FAST (3000 MWt)	Sodium	1986-1998
Phénix	France	233 FAST (590 MWt)	Sodium	1974-2009

The reactors listed in Table 4A were shut down due to challenges including public acceptance, high running cost, sodium leakages and fires, and fuel elements meltdown leading to abnormal rise in the sodium coolant temperature among others.

Table 4B: Liquid Metal Cooled Fast Reactors (LMFRs) In-operation

Reactor Name	Country	Power Level (MWe)	Coolant	Year of operation
BN-800	Russia	800 FAST	Sodium	2016 to date
BN-600	Russia	600 FAST	Sodium	1980 to date

Table 4C: Liquid Metal Cooled Fast Reactors (LMFRs) to Build Now

Reactor Name	Country	Power Level (MWe)	Coolant
BREST	Russia	300 FAST (300 LFR)	Lead

Table 4D: Liquid Metal Cooled Fast Reactors (LMFRs) to Build in Twenty to Twenty-Five Years

Reactor Name	Country	Power Level (MWe)	Coolant
PRISM	USA	622 FAST	Sodium

Terrapower	USA	600 FAST	Sodium
SVBR	Russia	100 FAST	Lead/bismuth
GEN 4	USA	25 FAST	Lead/bismuth

The efforts to build and operate LMFRs started with developments of various LMFR design concepts. These design concepts include SSTAR, SUPERSTAR and ABR of USA; ELSY, ALFRED and MYRRHA of EU; CLEAR-1 and SNCLFR of China; PEACER and PASCAR of South Korea; PBWFR and CANDLE of Japan; and BREST and SVBR of Russia. Other design concepts of LMRs include G4M, BREST-OD 300, SVBR-100, CLEAR-1, ELECTRA, SEALER, and ELFR (Zhang et al., 2019; Jeltsov, 2018). Several experimental and demonstration or prototype fast reactors have been built to help in guiding the design and construction of commercial fast reactors. These Experimental reactors include CEFR (China) 2010, 25 MWe; FBTR (India) 1985, 15 MWe; JOYO (Japan) 1977, 100 MWt; BOR 60 (Russia) 1968, 12 MWe; BR-5/BR-10 (Russia) 1958, 5-10 MW; FFTR (USA) 1980-2001, 400 MWt; EBR-II (USA) 1963-1994, 20 MWe; KNK-II (Germany) 1977-1991, 20 MWe; Rapsodie (France) 1967-1983, 40 MWt; Enrico Fermi (USA) 1963-1972, 61 MWe; LAMPRE (USA) 1961-1965, 1 MWt; EBR-I (USA) 1958-1963, 0.2 MWt; and Clementine (USA) 1946-1952, 25 kWt. These Demonstration or Prototype fast reactors include PFBR (India) 2011, 1250 MWe; BN-600 (Russia) 1980, 600 MWe; MONJU (Japan) 1995, restarted in 2010, 280 MWe; BN-350 (Kazakhstan) 1972-1999, 150 MWe; Super Phenix (France) 1985-1998, 1200 MWe; Phenix (France) 1973-1998, 250 MWe; and PFR (UK) 1974-1994, 250 MWe. Most of these reactors were liquid sodium cooled except EBR-1 and Clementine that were cooled using liquid sodium-potassium (NaK) and mercury (Hg) respectively (Dai et al., 2021).

SFR and LFR are the LMFR types that are mostly compared and other LMFR types are designed to have advantage over the base LMFR types (SFR and LFR) in comparison of how other LWR types are built to have advantage of the base LWR types (PWR and BWR). Table 5 summarizes the main differences between LWRs and LMRs from the safety viewpoint.

Table 5: Safety Characteristics of LWR and LMFR

Characteristics	LWR	LMFR
Core Geometry	Arranged in most reactive configuration	Not arranged in most reactive configuration
Pressure in primary system	High (about 15 MPa)	None (at 1 atm)
Chemical reaction potential	None	High (Na-air, Na-water)
Loss of coolant	Reactivity loss	Reactivity gain
Inherent heat removal capability	Low	High
Radiological Inventories Fission products Plutonium	Equivalent Medium	Equivalent High
Nuclear properties Beta β (pcm)	600-700 10-5	300-400 10-7

Alpha α (sec)		
----------------------	--	--

Application of liquid metal as coolant in the design and operation of NPPs has advantages and disadvantages just like light water-cooled reactors. These advantages include (Roelofs, 2018). The neutronic characteristics of liquid metals are such that neutrons created by fission in the fuel are not moderated, and a sufficient number of fast neutrons remains at disposal to keep the nuclear chain reaction going. Metals are liquid at the operating temperatures of the nuclear reactor with sufficient margin toward the evaporation point. Therefore, the system can be operated without pressurization in contrast to water-cooled reactors, and the reactors can be operated at low pressure.

Liquid metals typically possess good heat transport characteristics and high heat capacity allowing efficient transport of heat generated in the core with relatively small systems and providing grace time in case of accident situations. The high density of liquid metals relaxes the conditions for establishing natural circulation cooling loops in accident situations.

The high boiling point of liquid metals, at least above 850°C for sodium, mitigates issues with core voiding. For lead, the very high boiling point of about 1750°C practically prevents voiding in the core possibly leading to a clad failure, because the clad itself will have failed before the boiling point of lead is reached.

- A high efficiency for electricity production can be achieved by the application of liquid metal because of the relatively high operating temperatures that can be achieved.
- Compared with all other advanced nuclear reactor concepts, there is relatively large operating experience with liquid-metal-cooled reactors, especially with sodium-cooled reactors.
- The application of lead or lead-alloys as coolant allows integration of steam generators in the reactor vessel. For sodium alternative, secondary cooling options based on gas are being investigated.
- The heat transport characteristics of lead and lead-alloys allow large fuel rod pitches that result in low pressure drops and enable application of natural circulation.
- The high density of lead may induce, depending on the type of fuel, that molten fuel floats and thus in the case of a fuel melt near the core outlet moves in the direction of lower or no power.
- A lead or lead-alloy reactor pool ensures a high self-shielding capacity.

The disadvantages of application of liquid metal as coolant include. The typical high mass of liquid-metal-cooled systems (especially lead- and lead-bismuth cooled systems) requires special measures for seismic events. Corrosion issues may be always present, but they increase especially at temperatures above 600°C. When operating temperatures above 600°C are envisaged, which should in principle be beneficial especially for lead and lead-alloys, new materials need to be developed to withstand the corrosion issues. In-service inspection in opaque coolant is significantly more difficult than in transparent coolants like water and gases as optical inspection methods cannot be applied. Apart from that, the high density and elevated operation temperature of liquid metals create higher forces on inspection tools that therefore need to be specially developed and tested.

The high melting point of liquid metals requires preheaters and measures against solidification of the coolant in case of shutdown, both during normal operation and during accident situations. The high mass of lead and lead-alloys leads to erosion issues in the components of the primary cooling system. This limits the coolant speed in such

systems below 2m/s as a rule of thumb. The chemical reactivity of sodium with air and water requires a sealed coolant system and special measures to prevent (nuclear) consequences of such reactions. Typically, this involves multiple barriers between sodium and the environment. Also, it requires special care in the heat transfer from the primary sodium circuit toward the eventual energy conversion circuit. Mostly, an intermediate sodium loop is designed to prevent a chemical reaction between primary sodium and the water-steam loop of the energy conversion circuit. Obviously, this increases costs and at the same time leads to a loss of efficiency. Studies are ongoing to eliminate such an intermediate circuit.

During irradiation of lead-bismuth, highly radiotoxic polonium is produced that should be confined at all times. Tables 6 and 7 list the advantages and disadvantages of Sodium and Lead Cooled Fast Reactors (SFR and LFR).

Table 6: Advantages of SFR and LFR

SFR	LFR
Liquid metal coolants such as Sodium among others are weak neutron moderators compared to water as a much stronger neutron moderator	Instead of refueling, the whole core can be replaced after many years of operation. Such a reactor is suitable for countries that do not plan to build their own nuclear infrastructure.
Sodium melts at 371K and boils / vaporizes at 1156K, a difference of 785K between solid / frozen and gas / vapor states, compared to water with 100K as a temperature between ice and gas/vapor at normal, sea-level atmospheric pressure conditions making the liquid metal Sodium thermodynamically safe to operate than water.	As no electricity is required for the cooling after shutdown, this design has the potential to be safer than a water-cooled reactor. Liquid lead-bismuth systems can't cause an explosion and quickly solidify in case of a leak, further improving safety. Lead is very dense, and therefore a good shield against gamma rays .
The high temperatures reached by the coolant Sodium (the Phénix reactor outlet temperature was 560 C) permit a higher thermodynamic efficiency than in water cooled reactors.	Lead's nuclear properties allow it to prevent a positive void coefficient , which is difficult to prevent in large sodium fast reactor cores.
Sodium need not be pressurized since its boiling point is much higher than the reactor's operating temperature . Sodium does not corrode steel reactor parts.	The operating pressure is very low and lead has an extremely high boiling point of 1750 degrees Celsius, which is over 1100 degrees Celsius higher than the peak coolant operating temperature. This makes significant reactor pressurization by overheating virtually impossible.
Despite sodium's low specific heat (as compared to water), this enables the absorption of significant heat in the liquid phase, while maintaining large safety margins.	Lead does not react significantly with water or air, unlike sodium which burns readily in air and can explode in contact with water. This allows easier, cheaper and safer containment and heat exchanger/steam generator design.

Table 7: Disadvantages of SFR and LFR

SFR	LFR
A disadvantage of sodium is its chemical reactivity, which requires special precautions to prevent and suppress fires. If sodium comes into	Lead and lead-bismuth are very dense, increasing the weight of the system therefore requiring more structural support and seismic

contact with water it reacts to produce sodium hydroxide and hydrogen, and the hydrogen burns in contact with air. This was the case at the Monju Nuclear Power Plant in a 1995 accident	protection which increases building cost.
In addition, neutron capture causes it to become radioactive; albeit with a half-life of only 15 hours	While lead is cheap and abundant, bismuth is expensive and quite rare. A lead-bismuth reactor may require hundreds of tonnes of bismuth depending on reactor size.
There is high probability of sodium leaking and can easily burn in air and explode in contact with water	Solidification of the lead-bismuth solution renders the reactor inoperable.
	However, lead-bismuth eutectic has a comparatively low melting temperature of 125 °C, making desolidification a relatively easily accomplished task. Lead has a higher melting point of 327/328 °C, but is often used as a pool type reactor where the large bulk of lead does not easily freeze.
	External heating was required to keep a Lead-cooled fast reactor hot at all times to prevent solidification when it was turned off and not in use. An alternative was to keep the reactor in non-stop active running but doing this would result in increased mechanical wear, shortening the operational life.
	By leaking and solidifying, the coolant may damage the equipment.
	Lead-bismuth produces a considerable amount of polonium, a highly radioactive and quite mobile element. This can complicate maintenance and pose a plant contamination problem. Lead produces orders of magnitudes less polonium, and so has an advantage over lead-bismuth in this regard.

- For liquid metals, the Prandtl number, Pr, is less than 1 and the convective heat transfer coefficient (given in the Nusselt number, Nu) is a function of the Peclet number, $Pe = RePr$ where Re is the Reynolds number.
- Generally, for $Pe < 100$ heat transfer is dominated by heat conduction (Nu does not vary much with Pe) and is not affected by the coolant flow rate.
- The modest vertical elevation of the intermediate heat exchanger (IHX) relative to the core in a potential pool-type reactor design would make it less than ideal for establishing natural circulation flow in the primary system. Natural circulation depends on these elevations as well as hot and “cold” temperatures, and resistances in the loop.
- The relatively large mass of sodium in a pool-type reactor (versus a loop-type) provides large heat capacity to dampen temperature rise in off-normal transients but also influences the control and load following characteristics of the overall heat transport systems.
- No moderation in a fast spectrum core leads to a more compact core, that is, higher power density and higher specific power. This translates to more restrictive coolant flow passages and more severe heat removal requirements/constraints.
- High specific powers and power densities require large heat transfer areas and high heat transfer coefficients to be used to reduce fuel centerline and cladding temperatures and avoid melting.
- SFR fuel is typically in the form of small diameter tubes or fuel pins.
- Enhanced heat transfer from the fuel pins is facilitated by roughened cladding surfaces and turbulence promoters (e.g. wire-wrap spacers).
- A compact core makes core orificing more challenging but essential to counter the effects of power peaking.
- Testing performed at the Experimental Breeder Reactor-II (EBR-II) has demonstrated,
- metal fueled fast reactors can be self-protecting against anticipated transients without scram (ATWS)
- load-following control is manageable
- passive transition to natural convective core cooling
- passive rejection of decay heat
-

Thermal-Hydraulic and Neutronics Safety Characteristics of Sodium Cooled Fast Reactors

Thermal-Hydraulic Safety Characteristics

- From a thermal-hydraulics perspective, among the unique features of SFRs that have safety implications are their compact core size of relatively high-power density and the use of low-pressure sodium as primary coolant. The following characteristics are relevant:
- Liquid metals such as sodium (and potassium) have relatively low melting temperature (to avoid having to preheat the system to obtain a liquid coolant) and high boiling temperature (or low vapor pressure, to avoid boiling). They remain in liquid form over a wide range of temperatures.
- A pool-type reactor coupled with a low-pressure primary system makes the occurrence of a large loss-of-coolant accident (LOCA) unlikely, however leaks through instrumentation penetrations need to be considered.
- Operating at low pressures, sodium will not completely flash on depressurization. (Light water reactors are subject to system rupture followed by coolant depressurization on loss of coolant.)

From a neutronics perspective, among the unique features of SFRs that have safety implications are their compact core size, operation with a fast neutron spectrum, and utilization of Pu and higher enriched uranium (relative to thermal reactors) in the fuel. The following characteristics are relevant. Fast fission cross sections are a few hundred times lower than for thermal fissions requiring a higher concentration of fissionable fuel in a fast spectrum core. Smaller loss by parasitic capture in fuel and lesser poisonous effects from fission products lead to the possibility of higher fuel burnup and lower excess reactivity requirements for SFRs. With high burnups, good fission gas retention or venting becomes a major consideration in SFR fuel system design. Fuel burnup in SFRs is usually limited not by reactivity but by radiation damage to the fuel pins (e.g., swelling).

In general, the possibility of leakage of dense hydrogenous material into an SFR core must be avoided because of concern over prompt criticality brought on by positive reactivity associated with the softening of the neutron spectrum. SFRs generally have short prompt neutron lifetimes which may cause a large reactivity insertion rate in the event of a core disruption (core collapse) accident. In SFRs the effective delayed neutron fraction (β_{eff}) is impacted negatively by

Pu-239 (β for Pu-239 is only 0.00215 compared to 0.0068 for U-235) and positively by fast fission of the fertile U-238 ($\beta= 0.0158$).

SFRs are subject to positive void reactivity effects. The presence of void in the core reduces moderation (a positive reactivity effect) but also induces more neutron leakage (a negative reactivity effect). In small-sized SFRs, the effect of neutron leakage predominates over the effect of flux hardening. The situation is just the opposite for large-sized SFRs; significant flux hardening near core center and less predominant leakage near the core boundary. The general design philosophy for large-sized cores is to use special core design features, such as a pancake core with axial and radial blankets, to achieve a high-leakage core resulting in an overall negative sodium void reactivity. The presence of a harder neutron spectrum in metal-fueled SFRs leads to significantly smaller Doppler feedback than in ceramic-fueled reactors. Bowing of fuel assemblies due to radial temperature gradients across the core can lead to reactivity changes.

Additional Safety Concerns of Sodium Cooled Fast Reactors (SFRs)

Two concerns dominated the early safety analyses for fast spectrum reactors in the U.S., core compaction—due to slumping or melting—and prompt criticality. The core compaction issue originates from the fact that fuel densification would increase the system reactivity in contrast to the effect in thermal reactors. The prompt criticality concern is related to the small effective delayed neutron fraction and the short prompt neutron lifetime of an LMR. It is postulated in a hypothetical core disruptive accident (HCDA) that a core meltdown may rapidly lead to a prompt criticality condition with an extremely rapid power increase creating a potential energy release of magnitude larger than practically containable. Subsequent improvements have been made to the analytical techniques, most of which demonstrate reduced consequences from HCDA. Furthermore, HCDA generally is not a concern for metallic fuels; one of the drivers for their use rather than oxide fuels (Cheng et al., 2018).

Thermal-Hydraulic and Neutronics Safety Characteristics of Lead-Bismuth Eutectic and Lead Fast Reactors

The three liquid metals (Na, Pb and LBE) have some advantages over water or gas as coolant. For example, the three liquids metals have low pressure and good heat removal characteristics compared to that of water or gas as coolant (see Table 5). But there are some differences between lead and LBE coolants relative to Na coolant (Cheng et al., 2018). These differences in terms of thermal hydraulics include.

- Significantly higher boiling temperature for Pb/LBE – less likely to boil/void in transients/accidents
- High melting temperature for Pb – may require a heater to prevent freezing
- Low chemical activity with water, steam, air, water vapor – may avoid need for intermediate loop; facilitates having additional sources for cooling in accidents
- Lower neutron moderation allows larger pitch which enhances natural circulation
- Radiation resistant, low activation; however, polonium buildup with LBE may plate out throughout the primary coolant circuit -- presents a handling concern.
- Higher volumetric heat capacity
- Higher retention of fission products in Pb
- Higher density has impact on seismic events

- Erosion limits flow velocity relative to Na (velocity parameter in Table 2)
- Compatibility with structural components requires control of coolant oxygen and preservation of oxide coatings to minimize damage
- The Neutronics Safety Characteristics of Lead-Bismuth-Eutectic and Lead Fast Reactors include (Cheng et al., 2018):
- Lead/LBE reactors have neutron spectra close to that of SFRs but void coefficient of reactivity is of less an issue in Lead/LBE reactors which is not the case in SFRs.
- Lead/LBE reactors have lower neutron moderation ability which favors higher fission reactions. This couples with thermal hydraulics characteristics could allow larger pitch and hence favors natural circulation enhancement.
- Lead/LBE reactors have low burnup reactivity despite initial higher fissile inventory

Effects of Mixing of fluid flows at different temperatures

Studies on effects of fluid mixing in the reactor core to enhance fluid flow and heat transfer, and in the other T-Junction related parts of NPPs are found to be important and requires more attention to help us understand effects such as thermal fatigue, thermal stripping, thermal stratification, creep, corrosion and oxidation. These effects can be induced by temperature and pressure fluctuations. These types of studies on fluid mixing effects which are related to LM-cooled NPPs when performed can be compared with similar studies relating to water-cooled NPPs.

Studies involving mixing of fluid flows at different temperatures are mostly performed using CFD codes. Studies involving providing structures (mixing vanes as an example) in the path of fluid flow to enhance mixing and heat transfer are also mostly performed using CFD codes. These computational studies are also mostly validated using data obtained from experimental studies. Thermal fatigue as mentioned is one of the effects resulting from mixing of fluids. Thermal fatigue has always been a challenge when it comes to the mixing of fluid flows and researchers have been working for decades with regards to understanding and solving fatigue problems related to several spheres of thermal hydraulics and reactor management. Fatigue is also defined as the deterioration of material from the repeated cycles of thermal or mechanical loads or strains (OTA - E-575, 1993). thermal mixing is usually undertaken to homogenize the fluid properties and enhance heat and mass transfers and they contribute to thermal fatigue failure in nuclear power plants. Thermal mixing characterizes the phenomenon where hot and cold flow streams join, mix and result in temperature fluctuations. The temperature fluctuations cause cyclic thermal stresses and subsequent fatigue cracking of the pipe walls. Thus, the prediction of thermal field in a piping system is an important aspect from the nuclear reactor safety point of view. Thermal fatigue is a stress failure with macroscopic cracks resulting from cyclic thermal stresses and strains due to temperature changes, spatial temperature gradients, and high temperatures under constrained thermal deformation. Li et al., 2010 described thermal fatigue failures in cooling systems of reactors as the effects of the varying stresses on a piping system attributed to the mixing procedure of the cold and hot flows. *Thermal fatigue* is a particular kind of *fatigue* failure procedure caused by cyclic stresses from reiterative variations in the equipment's temperature. Besides, stated that temperature variations in areas where cold and hot flows are thoroughly mixed give rise to these stresses. also said mixing of fluids in a T-Junction turbulently can cause fluctuating thermal

stresses in pipe walls resulting into high cycle thermal fatigue. Thermal fatigue issue is a significant safety matter in question in managing thermal-hydraulic systems in nuclear power plants owing to the fact it can cause the pipe material to fail abruptly. Pointed it out that thermal fatigue failure in nuclear plants pipes are bound to happen when they are yielded to high cycle fatigue failure in the mixing regions. The failure happens because the cyclic qualities of the load which gives rise to microscopic material imperfections develop into a macroscopic crack also known as the initiation phase. Moreover, when it comes to understanding and managing of nuclear power plants ageing, thermal fatigue should be considered to ensure safety.

Eggerston, 2011 worked on the turbulent mixing and its effect on thermal fatigue. He stated that currently, several nuclear power plants across the world are approaching their actual stipulated existence of about forty years. He stated that there were measures being put in place to tackle the major issues that shorten their lifespan hence running of the current power plants can be maintained for longer thus up to sixty years and upcoming NPPs can be modeled with a longer lifespan. One of these main issues is thermal fatigue and the effects of thermal fatigue in power plants were shown by the failure of the residual heat removal loop in one of the reactors of the CIVAUX plant in France, an incident analyzed by Chapuliot with numerical analysis and with the European THERFAT project (Eggerston, 2011). They came to the conclusion with this investigation that thermal fatigue can deteriorate pipe walls in nuclear reactors and in the long-term cause primary coolant loss.

It is good to know that a lot of studies have been performed relating to mixing of fluid flows at different temperatures in a T-junction or related geometry using water as the fluid compared to similar limited studies performed using liquid metal as the fluid. Some of the main findings from the studies; performed using water as the mixing fluid are:

- Magnitude of thermal load could provide information on failures related to thermal fatigue.
- The magnitude of thermal load depends on temperature difference of mixing fluids.
- As the hydraulic diameter of the branch duct increases (velocity or momentum ratio decreases), the thermal load's magnitude reduces but the thermal load's intensity remains constant for constant flow conditions.
- Experimental studies involving PIV measurements are suitable for validation of CFD or related numerical studies on mixing of fluids at T-Junctions.
- CFD computations have capability to capture mixing fluid flow phenomena and the accompanied turbulent flow fluctuations in a T-junction.
- Dean vortices generated by a pipe bend have a crucial role in T-Junction thermal fatigue problems.

Parameters such as temperature, velocity, pressure, turbulent kinetic energy, density difference, thermal conductivity, stress intensity fluctuations, and power spectra density of temperature fluctuations among others could provide information on thermal fatigue resulting from mixing of fluid at T-Junction.

More experimental studies needed to be carried out to validate CFD and other related numerical studies on mixing of fluid flow phenomena as thermal fatigue and other related effects are major safety concerns in design and operation of NPPs.

A research that was performed using liquid metal as the mixing fluid was the study carried out Ferede (2020). The study made use of a pipe geometry, mercury as the mixing/working fluid and ANSYS 19.2 CFX as computational tool. The study investigated fluid behavior of fluid flowing in a T-junction pipe. It was found out that the velocity of a fluid at the branch of T-junction pipe has significant effect on the surrounding pressure, the pressure increases in the upstream whereas the pressure decreases in the downstream of the T-junction pipe. Thus, more studies have to be performed using liquid metal as the mixing fluid in a T-junction or related geometry to help us understand better the phenomenon of thermal fatigue relating to the use of liquid metal as a mixing fluid or as a coolant.

Experimental studies

Experimental studies are very crucial prior to the development, design and operation of fluid flow and heat transfer equipment for commercial utilization and purposes. These prototype experiments mainly provide design and operational data that guide the design and operation of commercial fluid flow and heat transfer equipment. These experimental data obtained from the experimental studies are also very crucial for the validation of Numerical and Computational Fluid Dynamics codes that are also used to provide data useful for design and operation of commercial fluid flow and heat transfer equipment. Thus, these prototype experiments provide basic data upon which commercial fluid flow and heat transfer equipment are developed, designed and operated safely.

This section provides information on some experimental studies carried out using liquid metal coolants. Liquid metal coolants transport the heat generated in the fuel rods for steam generation and power production. Thus, liquid metals are used as coolants in liquid metal cooled fast reactors (LMFRs). Table 8 provides information on some of experiments carried out using liquid metal coolants. The experiments are designed to study the behavior of liquid metal coolant, or study the interaction of liquid metal coolant with water, or to study the interaction of the liquid metal coolant with the fuel rod. Experimental facility, purpose of the experimental study and the main findings from the study are also stated in the Table 8. The experimental diagrams which are not provided in this review can be found in the mentioned references in the Table 8.

Table 8: Experimental studies carried out to investigate liquid metal coolant performance and/or coolant-coolant or coolant-fuel interaction.

S.No.	Experimental Facility/ Reference	Coolant; or (Coolant-Coolant or Coolant-Fuel interaction) Geometry of the test section	Purpose of the Experimental study and main findings from the experimental study
1	THEADES LBE test facility / Pacio et al., 2018	Lead-bismuth eutectic (LBE) coolant cooling the 19 rod bundle Geometry: 19-rod bundle hexagonal channel (Figure 4)	Purpose: To investigate internal flow blockages in LBE-cooled 19 rod bundles with wires spacers. Findings:

		<p>The LBE primary loop is cooled by the air secondary loop at the heat exchanger sections 5 and 6 of figures 4a and 4b.</p>	<p>i. An empirical model named Karlsruhe Blockage Equation (KBE) was proposed for representing the heat transfer resistance at the hottest spots in the blocked region for each element.</p> <p>ii. Extrapolating the results to full-power conditions, the temperature increase produced by solid blockages with low thermal conductivity could be acceptable if they were small and excessive if they were larger.</p>			<p>LBE, and S2 containing water to be injected into S1</p>	<p>Findings:</p> <p>i. The experimental results were modelled with SIMMER-III code and the obtained results show a pressure time trend in the reaction tank S1 in agreement with the experimental data during the whole transient.</p> <p>ii. The computed temperature time trends show a general cooling over estimation on the axis of S1.</p> <p>iii. Modelling of the two-phase pressure drop was key issue of consideration in order to get computational pressure time trends.</p>
2	LIFUS5 facility/ (Ciampichetti et al., 2009)	<p>lead-bismuth eutectic (LBE)-water interaction</p> <p>Geometry: an upper cylindrical part and a lower hemispherical part (S1 of Figure 5). S1 containing partially filled LBE, and S2 containing water to be injected into S1</p>	<p>Purpose: To investigate HLM (LBE) interaction with water (sub-cooled water at 7MPa and 235°C was injected into a reaction vessel containing LBE at 350°C).</p> <p>Findings: The simulation activity has highlighted the capability of SIMMER III to reproduce the interaction between LBE and water, even though the 2D feature of the code has represented the limitations in reproducing the experimental results.</p>				
3	LIFUS5/Mod2 facility/(Pesetti et al., 2015)	<p>Water-LBE interaction.</p> <p>Geometry: an upper cylindrical part and a lower hemispherical part (S1 of Figures 6a and 6b). S1 containing partially filled</p>	<p>Purpose: To investigate the water-LBE interaction (sub-cooled water at 40 bar and 240°C or 200°C was injected into a reaction vessel partially filled by low pressure LBE at 400°C).</p>				
4	CAS KYLIN 61-rod experimental facility/(Lyu et al., 2016)	<p>LBE coolant (primary loop) cooling the 61 rod bundle;</p> <p>Water coolant (secondary loop)</p> <p>Geometry: hexagonal duct/tube of 61 rod bundles, the heat source of Figure 7a and 7b. The primary loop of LBE is made up of the heat source (4); the water loop is part of the heat exchanger (7) for cooling LBE.</p>	<p>Purpose: To study the material corrosion, thermal hydraulics, and safety features of the lead-bismuth reactor; and to develop and verify sub-channel codes.</p> <p>Findings: The experimental results obtained under forced and natural circulation flows were successfully modelled with SACOS-PB sub-channel analysis code except the edge sub-channel coolant temperature under high mass flow rate case, with the reason attributed to the effect of wire wrap modeling.</p>				
5	Argonne's Metallic UraniumSafety	Uranium fuel-Sodium coolant interaction					<p>Purpose:</p>

	Experiment (MUSE) facility/Kim et al., 2020	Geometry: hexagonal channel/duct of 19 fuel pin bundle (Figures 8a and 8b)	<p>i. To investigate relocation behavior of uranium metallic fuel by conducting metallic fuel relocation experiments using 19-pin bundle test sections,</p> <p>ii. To measure pressure drop in order to evaluate the blockage of the sodium coolant channel.</p> <p>Findings: More formation of the eutectics could lead to more fuel dispersion and less blockage due to the lower freezing point of the eutectics</p>			<p>interface, while a thermal fragmentation event induced rapid vapor expansion.</p> <p>ii. Jet fragmentation was best explained by the vaporization of coolant entrained within the melt jet generating an internal over-pressure sufficient for fragmentation of the crust.</p> <p>iii. Thermal fragmentation produced missiles with velocities exceeding that of the jet, and a bimodal debris size distribution of coarse jet shells and finer fragments.</p>
6	VIPERE experiment/ David et al., 2019	Water coolant-Sodium coolant interaction Geometry: Pyrex beaker (Figure 9)	<p>Purpose: To investigate the runaway of sodium-water reaction</p> <p>Findings:</p> <p>i. The experimental results suggested that sodium vaporization was responsible for provoking Sodium-Water Reaction (SWR) runaway, and also was responsible for the onset of SWR runaway.</p> <p>ii. A semi-analytical model based on SWR mechanism was developed.</p>			
7	JAEA MELT facility/Johnson et al., 2021	Stainless steel cladding-Sodium coolant interaction Geometry: Closed bottom Opened top Cylindrical vessel (Figure 10)	<p>Purpose: To characterize jet quenching and fragmentation using a new software, SPECTRA</p> <p>Findings:</p> <p>i. The rebounding of melt fragments confirmed a solid outer crust at the melt-coolant</p>			
8	PMCI (Pressurization characteristics in Melt-Coolant Interaction) facility/Cheng et al., 2019	alloy (60% Bi, 20% In and 20% Sn) fuel-Sodium coolant interaction Purified water was used to simulate the sodium coolant. Geometry: Cylindrical vessel (Figure 11)	<p>Purpose: To investigate the effect of interaction mode on local FCIs adopting Melt-Injection (MI) mode instead of Coolant-Injection (CI) mode (MI is fuel-alloy injection into Sodium, CI is water injection into Sodium).</p> <p>Findings:</p> <p>i. Mechanical energy conversion efficiency was much lower within the MI-mode condition compared to Coolant-Injection (CI) mode condition.</p> <p>ii. Additional experimental data was provided for verifications of fast reactor safety accident analysis codes.</p>			
9	MOX-LBE interaction experiment/	uranium plutonium mixed oxide				<p>Purpose: To study interaction</p>

	Vigier et al., 2015	(MOX) pellets fuel - molten lead bismuth eutectic (LBE) coolant interaction Geometry: Cylindrical containers with upper and lower chambers (Figure 12)	between uranium plutonium mixed oxide (MOX) fuel pellets and - molten lead bismuth eutectic (LBE) coolant. Findings: i. The MOX fuel pellets integrity was preserved in all the cases of adverse conditions considered for 50 hours of interaction, neither the interaction compounds (crystalline or amorphous) nor lead and bismuth diffusion into the surface regions of the MOX pellets was detected. ii. The amounts of different actinides released from MOX fuel pellets into the LBE coolant were limited (in the range of 0.01-0.15 mg).			of the rapid and complex phenomena of a metal-gas-liquid mixture.	
10	LBE-Water interaction experiment/ (Nakamura et al., 1999)	Pb-Bi alloy (LBE)-Water interaction Geometry: Cylindrical vessel with a hemispherical bottom (Figure 13)	Purpose: i. To observe the behavior of a high-temperature (~773 K) molten Pb-Bi alloy dropped into a vessel containing water or into an empty, thin (~10 mm) thick vessel; ii. To observe molten Pb-Bi alloy dropped into a vessel containing high-temperature pool water (~373 K) Findings: The visualization technique (PIV) adopted proved to be a promising tool for observation and measurement	11	Water-LBE interaction experiment/ (Sibamoto et al., 2002; Sibamoto et al., 2007)	Water-Pb-Bi alloy (LBE) interaction Geometry: Cylindrical vessel with a hemispherical bottom (Figure 14)	Purpose: i. To observe and measure the penetration behavior of plunging water jet in a high-temperature (~823 K) molten lead-bismuth alloy liquid pool. ii. To investigate the transient thermal and hydraulic conditions of water jet into molten lead-bismuth pool. Findings: i. The termination of the water cavity penetration is determined primarily by the stability of the subcooled film boiling on the melt/water interface. ii. The increase in water temperature triggers the onset of unstable boiling instead of stabilizing the film boiling. iii. The maximum penetration length is limited by the buoyancy for low-Froude number experiments with a large melt-to-jet density ratio (R), which is contrary to high-Froude number with low-R cases, where the penetration is limited by jet breakup iv. Boiling increases thrust force on the cavity surface by increasing the momentum

of outflow from the cavity

v. The onset of bulk boiling of the water in the cavity causes an upward expulsion of water from the cavity, and the cavity depth and volume approach their final asymptotic values

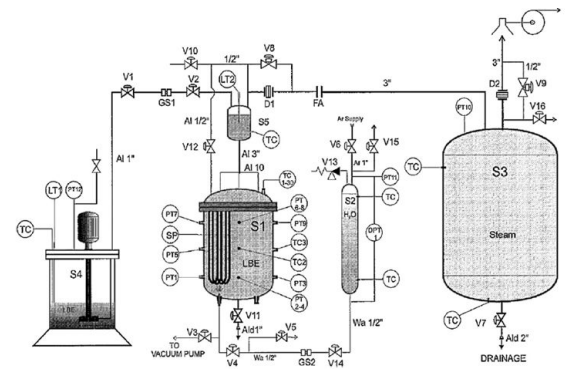


Figure 5: Schematic representation of LIFUS 5 facility (Ciampichetti et al., 2009) S1, Reaction tank; S2, Water tank; S3, Safety/dump tank; S4, Liquid metal storage tank; S5, Expansion tank

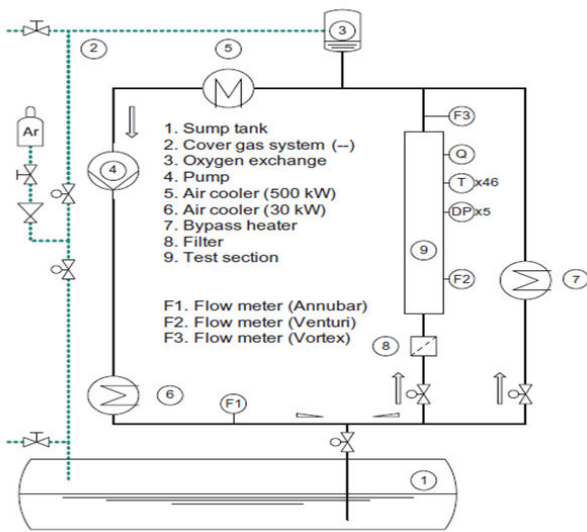


Figure 4a: Simplified diagram of THEADES LBE test facility (Pacio et al., 2018)

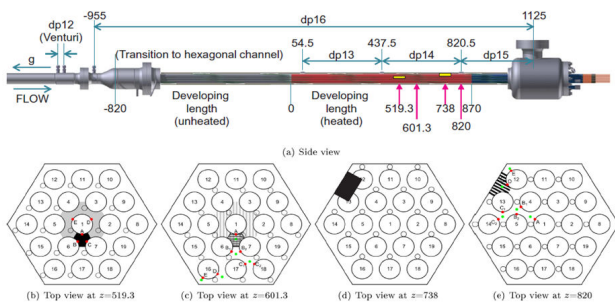


Figure 4b: Test section (all lengths in mm refer to the onset of the heated zone) (Pacio et al., 2018)

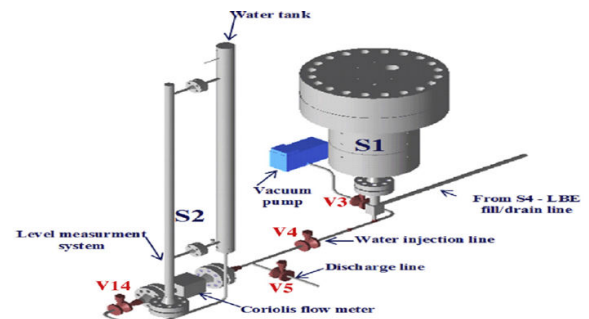


Figure 6a : LIFUS5/Mod2 overall sketch (Pesetti et al., 2015)

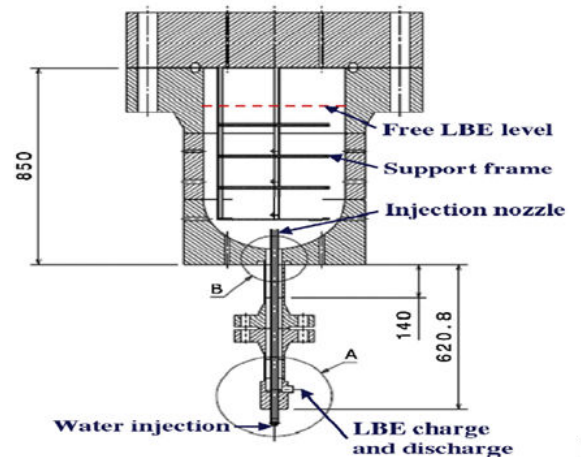


Figure 6b: LIFUS5/Mod2 facility, injection system (Pesetti et al., 2015)

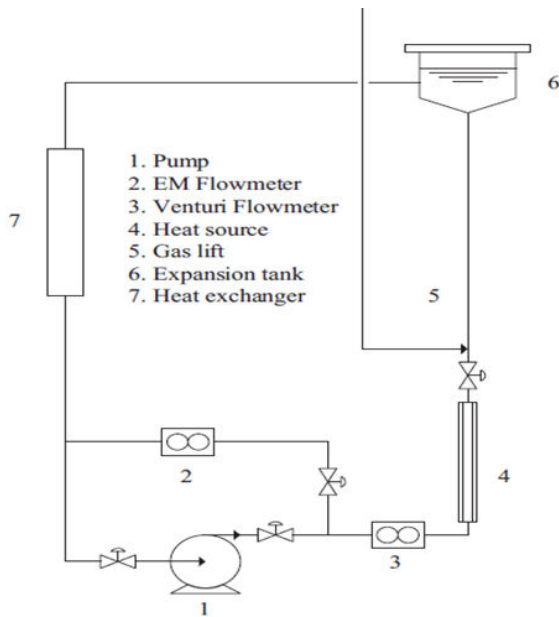


Figure 7a: The general layout of CAS KYLIN-II mixed circulation loop (Lyu et al., 2016)

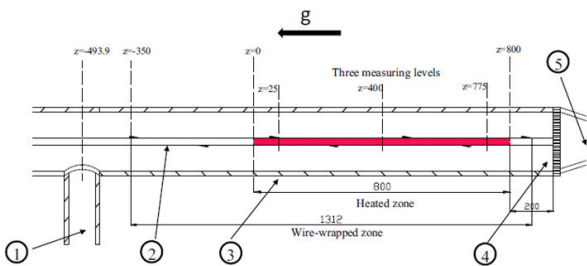


Figure 7b: Schematic diagram of the test section

1 – Inlet zone; 2 – Fuel pin simulator; 3 – Hexagonal tube; 4 – Upper support grid; 5 – Outlet zone (Lyu et al., 2016)

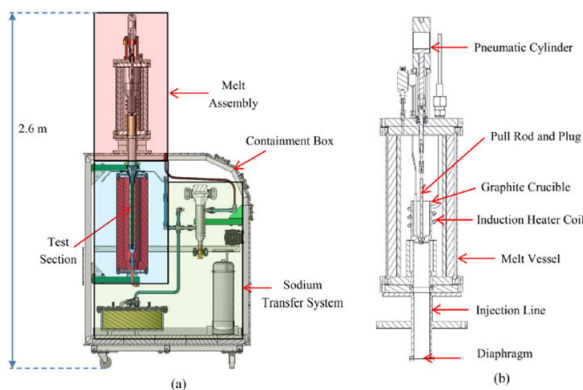


Figure 8a: Schematic of Metallic Uranium Safety Experiment (MUSE) facility (b) melt assembly (Kim et al., 2020)

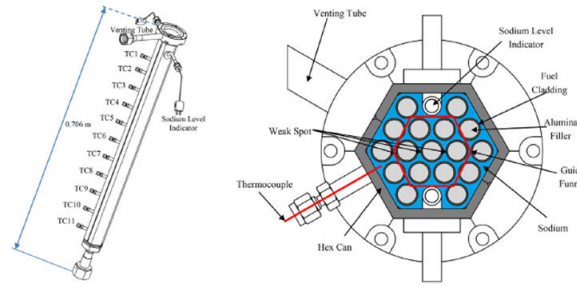


Figure 8.b: Schematic diagrams of pin bundle test section (Kim et al., 2020)

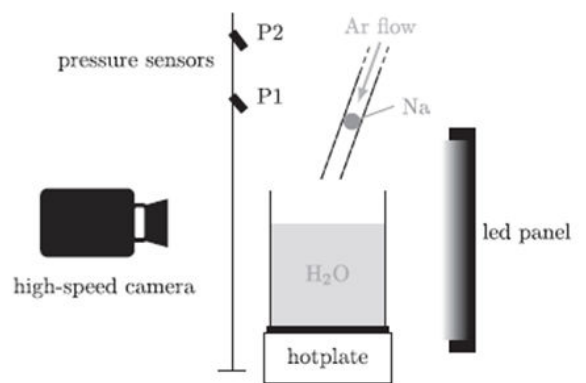


Figure 9: Schematic representation of VIPERE experimental setup. A 1 g spherical solid sodium pellet is put in contact with liquid water. The reaction is filmed using a high-speed camera (David et al., 2019).

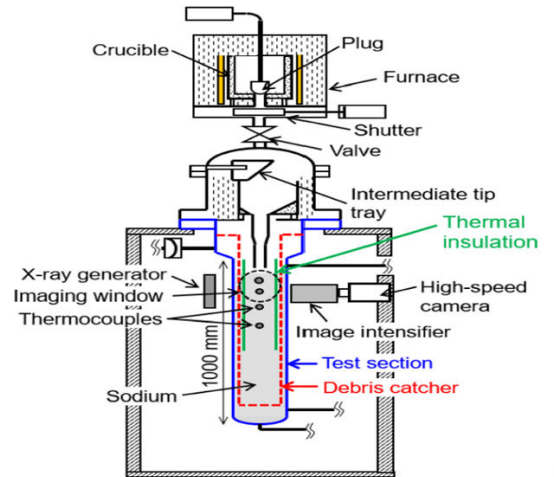


Figure 10: Schematic of the MELT facility as configured for the FCINA-30-1 test, modified from Matsuba et al., 2016 (Johnson et al., 2021).

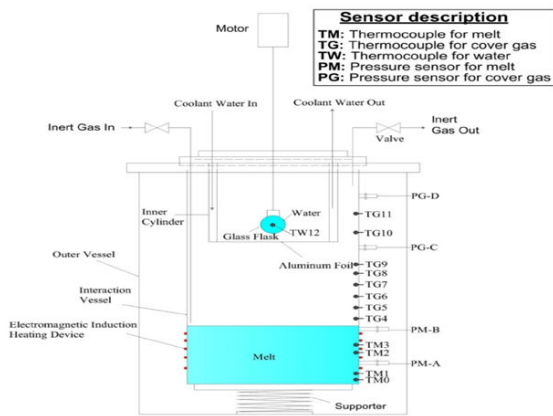


Figure 11: Schematic diagram of the Pressurization characteristics in Melt-Coolant Interaction (PMCI) facility developed at Sun Yat-sen University (SYSU).

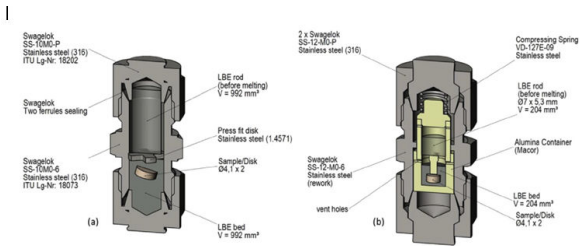


Figure 12: Sketch of the containers used for the interaction tests: (a) metallic container made of stainless steel used for interaction tests with low oxygen content in LBE and (b) alumina

container used for the interaction tests with high oxygen content in LBE integrated in Swagelok vessel to ensure tightness.

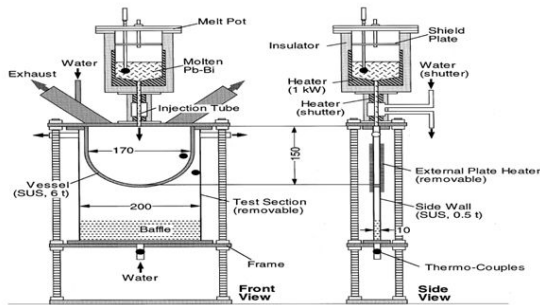


Figure 13: Schematic of test rig

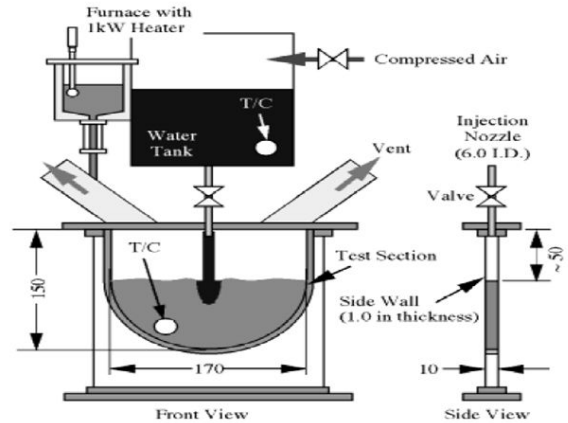


Figure 14 : Schematic view of test apparatus

Computational studies

Computational studies using codes including computational fluid dynamics CFD codes among other computational codes are very helpful in different research areas because results obtained using these CFD codes are comparable to that of experimental studies. More detailed results that cannot be obtained through experimental studies can be obtained using CFD codes. Therefore, computational studies are needed to provide further understanding of results obtained through experimental studies, and therefore guide the design and operation of many industrial equipment.

Table 9 provides information on computational studies carried out using liquid metal coolants. The computational tool, geometry and coolant adopted, purpose and main findings of the respective studies are provided in the Table 9. The details of these computational studies can be found in the references provided in the table 9.

Table 9: Computational studies carried out using various computational tools/codes

	Study/ Reference	Computational tool/ code adopted	Geometry/ Coolant adopted	Purpose and main findings of the study
1	Ferede, 2019	ANSYS 19.2 CFX	Pipe/ mercury	<p>Purpose: To investigate fluid behavior of fluid flowing in a T-junction pipe.</p> <p>Findings: It was found out that the velocity of a fluid at the branch of T-junction pipe has significant effect on the surrounding pressure, the pressure</p>

				increases in the upstream whereas the pressure decreases in the downstream of the T-junction pipe.				friction coefficient have a direct relationship on the drop time. The drop time estimation directly relates to the LBE density, mass flow rate and friction coefficient
2	Arthur et al., 2020	MATLAB	CRA and hexagonal guide tube geometry assumed cylindrical/LBE	<p>Purpose: To perform drop dynamics analysis of control rod assembly in a LBE-cooled research reactor.</p> <p>Findings:</p> <p>i. The CLEAR-I CRA drop time at the normal operating condition was found to be 576.8 ms with a drop velocity of 2.81 m/s.</p> <p>iii. Although, differential pressure and viscous resistance contribute well to the LBE hydraulic resistance, the contribution from the LBE buoyancy dominates due to the characteristic high density of the LBE.</p> <p>LBE hydraulic resistance depends on differential pressure, viscous resistance, and LBE buoyancy</p> <p>v. The LBE density, mass flow rate and</p>				vi. The total CRA mass has negative relationship with the drop time and influences it significantly. The CRA mass negatively relates to the drop time.
3	Jeong et al., 2020				ANSYS-CFX, Flow visualization experiments using a combined PIV and MIR technique also performed.	hexagonal duct of sub-channel and wire-wrapped pins/Sodium		<p>Purpose: To investigate effects of flow mixing wire spacers and develop U-pattern wire spacer for enhanced heat transfer and reduced pressure drop.</p> <p>Findings:</p> <p>i. The U-pattern spacer was compared with conventional wire spacer.</p> <p>ii. The effect of reduced pressure was large under high flow rate condition, $Re > 10,000$ using the U-pattern wire spacer.</p>

				<p>iii. The U-pattern wire spacer was found to have enhanced heat transfer effects and thereby reducing peak cladding temperature as well as reducing pressure drop by 8.6°C and 5.2% respectively.</p>				<p>used in existing LMFBR thermal hydraulic analysis codes.</p> <p>iv. The results of turbulent flow characteristics of inter-wrapper channel and rectangular channel were almost the same but different for the laminar flow characteristics of the two channels.</p>
4	Liang et al., 2021	FORTRAN 95, ANSYS-FLUENT, Experimental study also performed	Inter-wrapper flow channel/ Liquid metal (LM)	<p>Purpose: To investigate flow characteristics of inter-wrapper channel in LMFBR.</p> <p>Findings:</p> <p>i. New pressure drop correlations for inter-wrapper flow channels with different aspect ratios were developed.</p> <p>ii. Friction factor estimated for inter-wrapper channel and circular tube in turbulent regime were almost the same but significantly different in laminar regime.</p> <p>iii. The results of the friction factor correlations developed in this study were not the same as for those correlations</p>				
5	Liu et al., 2019				STAR-CCM + (CFD), COBRA-YT (subchannel) was also used for purpose of comparison.	hexagonal sub-channel and 61-pin fuel assembly/LBE	<p>Purpose: To investigate various blockage conditions of lead-bismuth eutectic-cooled fuel assembly.</p> <p>Findings: The results indicated that the cladding temperature during a blockage accident should be evaluated to avoid exceeding the design criteria.</p>	
6	Natesan and Velusamy, 2019				Coupled code DYANA-HM (CFD code STITH-2D and one dimensional code DYANA-P coupled)	Reactor core, single primary and secondary circuits of a pool type fast reactor/ Sodium	<p>Purpose: To investigate plant transients in sodium cooled fast reactors.</p> <p>Transients in which heat removal through steam generators is available, and is not available is investigated.</p>	

				<p>Findings: The results showed effects of thermal stratification in hot pool should be considered in the development of computational prediction codes for realistic prediction of temperature evolution in the entire plant. Thermal stratification effects in hot pool was also found to affect evolution of natural convection flow in the secondary sodium circuit.</p>					<p>iii. The temperature distribution in different regions of the ESCAPE pool is well predicted within 10% with the measurements.</p> <p>iv. the effect of decreasing mass flow rate with temperature in the ESCAPE pool is well predicted.</p>
7	Visser et al., 2020	STAR-CCM + cfd code	<p>Cylindrical reactor vessel of ESCAPE/ lead-bismuth-eutectic (LBE)</p> <p>ESCAPE is a thermal hydraulic 1/6th-scale model of the MYRRHA reactor</p>	<p>Purpose: To model the flow and heat transport in ESCAPE using the Computational Fluid Dynamics (CFD) code STAR-CCM +</p> <p>Findings: i. The pressure drop from inlet to outlet of the ESCAPE pool is about 20% over-predicted by the CFD model. ii. The heat loss from the outer vessel wall of ESCAPE to the environment is predicted with about 5% accuracy.</p>		Jeltsov et al., 2018	STAR-CCM + cfd code	Cylindrical reactor vessel of ELSY reactor/lead	<p>Purpose: To study seismic sloshing in ELSY reactor in order to evaluate the effects of seismic isolation system on sloshing at different levels of earthquake.</p> <p>Findings: i. Partitioning baffles implemented in the free surface region between SGs were proposed as a potential mitigation measure to further reduce the sloshing loads to safe levels. ii. The reduction of loads by SI is not sufficient to reduce the sloshing loads to safe levels. iii. The flow congestion in the gap between</p>

				<p>respectively .</p> <p>v. The DES model results of the Nusselt number along the channel were consistently higher than those calculated using the k-ω and the k-ϵ models</p>					<p>the turbulent mixing and the turbulence kinetic energy. v. The vortex core has a high cladding wall temperature, and the attachment line has a low cladding wall temperature</p>
11	Jeong and Song 2021	ANSYS CFX cfd code	hexagonal channel of 7-pin fuel assembly/ Sodium	<p>Purpose: To investigate flow blockage of a JAEA 7-pin fuel assembly cooled with sodium</p> <p>Findings:</p> <p>i. Multi-scale vortices developed in axial direction were found around the blockage. ii. The blockage plate and grid spacer increase the pressure drop (friction factor) to about 36% compared to the bare case. and 12% for the case with blockage plate; iii. Formation of vortex increased the pressure drop. iv. The small-scale vortex structures significantly enhance the convective heat transfer because it increases</p>					

control rod assembly (CRA); particle image velocimetry (PIV); matching index-of-refraction (MIR)

Turbulence models and near wall treatment models available in ANSYS CFX and FLUENT CFD codes

Among other factors that determine the accuracy of predictions after the geometry is modeled are the selection/choice of particular turbulence model and the corresponding appropriate near-wall treatment model. And It is obvious that the way and manner turbulence is modeled in the regions near the wall will be different from the regions far away from the wall. Fluid flows through both industrial and non-industrial equipment/systems are predominantly turbulent and mostly wall-bounded. These turbulent flows are well modelled using turbulence models and near-wall treatment models which are Wall Function models (Wall Function Method/Approach) or Low-Reynolds modelling (see Tables 10, 11, 12 and 13). Table 10 lists turbulence models in FLUENT and CFX, Table 11 lists near wall function treatment models in available in FLUENT and CFX for Wall Function Method/Approach, and Tables 12 and 13 compare Wall Function Method or Low-Reynolds modelling Method respectively in FLUENT and CFX. The Wall Function method uses empirical formulas that impose suitable conditions near to the wall without resolving the boundary layer, thus saving computational resources. The Low-Reynolds Modeling method resolves the details of the boundary layer profile by using very small mesh length scales in the direction normal to the wall (very thin inflation layers). The computations are extended through the viscosity-affected sublayer close to the wall. The low-Re approach requires a very fine mesh in the near-wall zone and correspondingly large number of nodes. Computer-storage and runtime requirements are higher than those of the wall-function approach and care must be taken to ensure good numerical resolution in the near-wall region to capture the rapid variation in variables (see Figures 15 and 16).

The wall Yplus (y^+) value is used as a guide in selecting particular turbulence model with respect to the choice of wall treatment model associated with Wall Function or Low-Reynolds Modeling method. That is determination of the near-wall-mesh size/resolution (or y^+ value) required by Wall Function Method or Low-Reynolds Modeling Method of near wall treatment will inform the choice of a particular Turbulence Model. The wall y^+ is a non-dimensional distance similar to local Reynolds number, often used in CFD to describe how coarse (for high values of y^+) or fine (for low values of y^+) a mesh is for a

particular flow. It is the ratio between the turbulent and laminar influences in a cell (Salim and Cheah, 2009). The y^+ is the dimensionless distance from the wall and is also based on the shear stress. Y^+ is used to check the location of the first node away from a wall (ANSYS, 2005).

The turbulence models available in FLUENT include Spalart-Allmaras (1 eqn); k-epsilon (2 eqn) [Standard, RNG, Realizable]; k-omega (2 eqn) [Standard, SST]; Transition k-l-d-omega (3 eqn); Transition SST (4 eqn); Reynolds Stress (7 eqn); Scale-Adaptive Simulation (SAS); Detached Eddy Simulation (DES); and Large Eddy Simulation (LES) of which Spalart-Allmaras; k-epsilon; k-omega; Transition k-l-d-omega; Transition SST; and Reynolds Stress (7 eqn) are Reynolds Averaged Navier-Stokes (RANS) based turbulence models, and Scale-Adaptive Simulation; Detached Eddy Simulation; and Large Eddy Simulation are Scale-Resolving Simulation (SRS) turbulence models. SRS refers to all turbulence models, which resolve at least a portion of the turbulence spectrum in at least a part of the domain.

RANS turbulence models generally consists of zero-equation models, one-equation models, two-equation models, and stress equation models. In fluid dynamics, turbulent flow is the movement of fluid embodied by chaotic variations in pressure and flow velocity. In modeling turbulent flows, the Reynolds-averaged Navier-Stokes equations (RANS) are mostly used because they do not break apart turbulent structures with respect to time and location but rather model the important parameters through a turbulent kinetic energy perspective and this is a relatively fast method that often produces good results (Alfonsi, 2009). There are generally three approaches for turbulence modeling, Direct Numerical Simulation (DNS), Reynolds-Averaged Navier Stokes (RANS), and Large Eddy Simulation (LES).

Table 10: Comparison of Turbulence Models in ANSYS FLUENT and CFX cfd codes

ANSYS FLUENT cfd	ANSYS CFX cfd
Turbulence Models	Turbulence Models
Spalart-Allmaras (1 eqn)	The Zero Equation Model
k-epsilon (2 eqn) [Standard, RNG, Realizable]	The k-epsilon Model
k-omega (2 eqn) [Standard, SST]	The RNG k-epsilon Model
V2F *	The k-omega and SST Models [The Standard k- ω , BSL k- ω and SST k- ω Models]
Reynolds Stress (7 eqn)	The Reynolds Stress Model
Transition k-l-d-omega (3 eqn)	Omega-Based Reynolds Stress Models
Transition SST (4 eqn)	Explicit Algebraic Reynolds Stress Model
Scale-Adaptive Simulation (SAS)	CFX Transition Model
Detached Eddy Simulation (DES)	The Large Eddy Simulation Model (LES)

Large Eddy Simulation (LES)	The Detached Eddy Simulation Model (DES)
	The Scale-Adaptive Simulation (SAS)

BSL (baseline); SST (shear stress transport)

*V2F is an embedded add-on functionality in FLUENT which requires a separate license from Cascade Technologies (ANSYS 2010).

Table 11 : Comparison of models in Wall Function approach/method of treating turbulence near the wall in ANSYS FLUENT and CFX cfd codes.

Wall Function models available in FLUENT	Wall Function models available in CFX
Standard Wall Functions ($30 < y^+ < 300$)	Standard Wall Functions
Scalable Wall Functions ($y^+ > 11.225$)	Scalable Wall Functions ($y^+ = 11.067$ for near wall refine mesh, $y^+ \approx 20-200$ for outer wall coarse mesh, refer to Table 13 for details)
Non-Equilibrium Wall Functions ($30 < y^+ < 300$), refer to Table 12 for additional details	Automatic Near-Wall Treatment for Omega-Based Models ($y^+ \approx 1$ for near wall refine mesh, $y^+ \approx 20-200$ for outer wall coarse mesh, refer to Table 13 for details)
Enhanced Wall Treatment ($y^+ < 5$)	User Defined Wall Functions
User-Defined Wall Functions	

Table 12 : Comparison of Wall Function and Low-Reynolds Modeling methods in ANSYS FLUENT CFD code

Using a Wall Function	Resolving the Viscous Sublayer (Low-Reynolds Modeling)
The standard and non-equilibrium wall functions are options for all of the k- ϵ turbulence models as well as the Reynolds stress turbulence model.	First grid cell needs to be at about $y^+ = 1$ This will add significantly to the mesh count, require more computational power
Scalable wall functions are applicable for all high-Reynolds-number turbulence models (non k-omega (k- ω) models which are low-Re-models)	Use a low-Reynolds number turbulence model (like k-omega)
The Enhanced Wall Treatment (EWT) option is available for the turbulence models, k- ϵ and Reynolds Stress Model (RSM) models (EWT is the sole treatment for Spalart Allmaras and k- ω models).	Suitable if the forces or heat transfer on the wall are key to the simulation (aerodynamic drag, turbomachinery blade performance, heat transfer). The recommended turbulence model for most cases is SST k- ω (ANSYS, 2006, 2015)
First grid cell needs to be $30 < y^+ < 300$ for Standard and Non-Equilibrium Wall Functions. The model is invalid if y^+ is too low. The wall is not properly resolved if y^+ is too high. Refer to Table 11 for specific y^+ values for Wall Function types. Wall functions should never be used if $y^+ < 3$	

<p>Make the mesh either coarse or fine enough to avoid placing the wall-adjacent cells in the buffer layer ($5 < y^+ < 30$).</p> <p>The wall function is not applicable for all the turbulence models</p> <p>Suitable if more interested in the mixing in the middle of the domain, rather than forces on the wall (ANSYS, 2006, 2010).</p>	
--	--

Table 13: Comparison of Wall Function and Low-Reynolds Modeling methods in ANSYS CFX CFD code

Using a Wall Function	Resolving the Viscous Sublayer (Low-Reynolds Modeling)
<p>Standard Wall Functions</p> <p>Mesh with $20 \leq y^+ \leq 200$</p> <p>k-ε turbulence models</p> <p>Standard wall functions have been replaced by scalable wall functions as the default but standard wall functions are still available for backward compatibility of the code. Using standard wall functions are not recommended, as they offer no advantage over the scalable wall functions.</p>	<p>Highly refine mesh with $y^+ \leq 1$</p> <p>Turbulence models based on the ω-equation, such as the SST or SMC-ω models, are suitable for</p> <p>A low-Re method. Note that the low-Re method does not refer to the device Reynolds number, but to the turbulent Reynolds number, which is low in the viscous sublayer</p> <p>Low-Re models are in this case fine mesh solutions of the k-ω models (which includes the SST model). The k-ω models do accept coarser meshes, due to the automatic near-wall treatment for these models (ANSYS, 2006, 2015).</p>
<p>Scalable wall functions</p> <p>k-ε models</p> <p>No switch. Wall-adjacent vertices should be in the log-law layer: $y^+ \approx 20-200$</p> <p>In highly refined mesh, the first vertex is shifted virtually to $y^+ = 11.067$, linear to logarithmic transition.</p> <p>Further refinement near the wall has no effect.</p>	
<p>Automatic wall functions</p> <p>ω-based turbulence models, e.g. SST</p> <p>Switches between wall function & low-Re wall treatment as mesh is refined</p> <p>Wall-adjacent vertices should be in the log-law layer: $y^+ \approx 20-200$</p> <p>Wall-adjacent vertices should be within the viscous sublayer, $y^+ \approx 1$ with a minimum of 10 nodes in boundary layer</p>	
<p>All turbulence models in CFX are suitable for a wall function method (ANSYS, 2006, 2010).</p>	

Shear Stress Transport (SST); Second-Moment Closure (SMC)

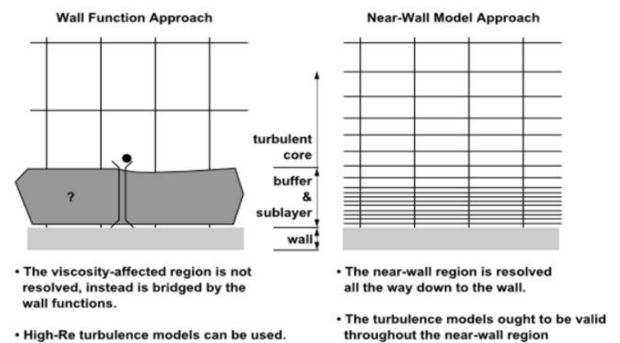


Figure 15: Wall Function approach and Near-Wall Model approach (Low-Reynolds Modeling) of wall-bounded turbulent flows (ANSYS, 2006)

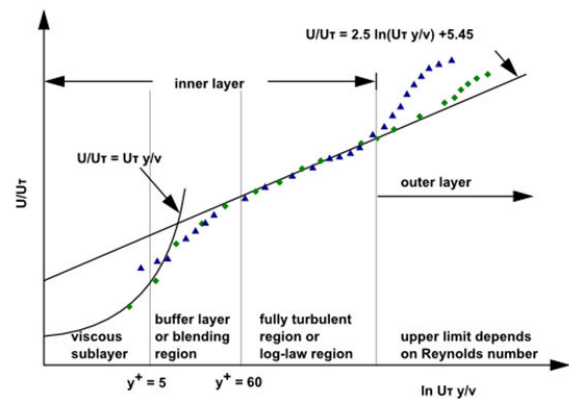


Figure 16 : Composite regions of the turbulent boundary layer (ANSYS, 2010)

Turbulence Models and Wall Treatment Models available in STAR-CCM+ CFD code

Table 14a and 14b show various wall treatments associated with turbulence models available in STAR-CCM+ CFD code [1,2].

A wall treatment in STAR-CCM+ is the set of near-wall modeling assumptions for each turbulence model. The wall treatments have been specialized according to each turbulence model, since assumptions specific to that model must be made for the wall boundary conditions for the turbulence quantities. The three types of wall treatment provided in STAR-CCM+ include high-, low- and all- wall treatments [2].

The high- wall treatment which implies the wall-function-type approach, assumes that the near-wall cell lies within the logarithmic region of the boundary layer.

The low- wall treatment is suitable only for low-Reynolds number turbulence models: this treatment assumes that the viscous sublayer is properly resolved.

The all- wall treatment is a hybrid treatment that attempts to emulate the high- wall treatment for coarse meshes, and the low- wall treatment for fine meshes. It is also formulated with the desirable characteristic of producing reasonable answers for meshes of

intermediate resolution (that is, when the wall-cell centroid falls within the buffer region of the boundary layer).

Table 14a: Reynolds-Averaged Turbulence models with their Wall Treatments

Reynolds-Averaged Turbulence models		
Turbulence Models	Different Types	Wall Treatments
K-Epsilon Turbulence	Standard K-Epsilon	High y+ Wall Treatment
	Standard K-Epsilon Low-Re (LIEN)	All y+ Wall Treatment
		Low y+ Wall Treatment
	Standard K-Epsilon Two-Layer	All y+ Wall Treatment
	Realizable K-Epsilon	High y+ Wall Treatment
	Realizable K-Epsilon Two-Layer	All y+ Wall Treatment
		Low y+ Wall Treatment
	AKN K-Epsilon Low-Re	All y+ Wall Treatment
		Low y+ Wall Treatment
	EB	All y+ Wall Treatment
Low y+ Wall Treatment		
V2F	All y+ Wall Treatment	
	Low y+ Wall Treatment	
K-Omega Turbulence	Standard (Wilcox) K-Omega model	High y+ Wall Treatment
		All y+ Wall Treatment
		Low y+ Wall Treatment
	SST (Menter) K-Omega model	High y+ Wall Treatment
		All y+ Wall Treatment
		Low y+ Wall Treatment
Reynolds Stress Turbulence	Linear Pressure Strain	High y+ Wall Treatment
	Linear Pressure Strain Two-layer	Two layer All y+ Wall Treatment
	Quadratic Pressure Strain	High y+ Wall Treatment
	Elliptic Blending	All y+ Wall Treatment
Spalart-Allmaras Turbulence	Standard Spalart-Allmaras	All y+ Wall Treatment
		Low y+ Wall Treatment
	High-Reynolds number Spalart-Allmaras	High y+ Wall Treatment

Table 14b: Large Eddy and Detached Eddy Turbulence models with their Wall Treatments

Large Eddy and Detached Eddy Turbulence models
--

Turbulence Models	Different Types	Wall Treatments
Large Turbulence Eddy	Dynamic Smagorinsky Subgrid Scale	All y+ Wall Treatment
		Low y+ Wall Treatment
		All y+ Wall Treatment
	Smagorinsky Subgrid Scale	All y+ Wall Treatment
		Low y+ Wall Treatment
	WALE Subgrid Scale	All y+ Wall Treatment
Low y+ Wall Treatment		
Detached Turbulence Eddy	EB K-Epsilon	All y+ Wall Treatment
		Low y+ Wall Treatment
	Spalart-Allmaras	All y+ Wall Treatment
		Low y+ Wall Treatment
	SST (Menter) K-Omega	High y+ Wall Treatment
		All y+ Wall Treatment
		Low y+ Wall Treatment
		Low y+ Wall Treatment

Comparing selection of turbulence model in STAR-CCM+ with that of ANSYS FLUENT or CFX, the wall treatment models of High y+, All y+ and Low y+ are associated with each turbulence models in STAR-CCM+ whereas in ANSYS FLUENT or CFX, one must first have knowledge on the mesh size/resolution (y+ value) which informs the choice of wall treatment model of Wall Function method or Low-Reynolds Modeling method and hence the choice of the turbulence model type. Zhang et al., 2019 provided detailed list of heat transfer correlations in triangular, tube and rod bundle geometries which are applicable for LMFRs. Other correlations including correlations for annular channels have also been provided by Zhang et al., 2019. These correlations are implemented in the computational codes for performing fluid flow and heat transfer analysis.

Research concerns of LMFRs

Reactor systems have specific research concerns that are well studied and enough data provided to help the design and operation of these reactor systems. PWR systems have concerns of nucleate boiling margin, departure from nucleate boiling ratio, critical heat flux, etc.; BWR systems have concerns of critical heat flux (critical heat flux ratio), flow instability, etc.; and SCWR systems have concerns of flow instability and natural circulation, depressurization and choked flow, etc.; just to mention a few. LMFR systems also have research concerns that have been mentioned in this section.

Mentioned that thermal-hydraulic issues are related to reactor core, pool and systems as shown in Figures 17, 18, and 19. Some specific research concerns of LMFR systems that are related to thermal hydraulics (reactor core, pool, systems), reactor neutronics, and accident scenarios are mentioned briefly below.

Thermal-hydraulics challenges are related to the CORE (Fuel assembly, Complete core modelling, Control rod behavior, Flow blockages, Inter wrapper flow, molten fuel relocation and refreezing, lack of analysis tools); POOL (Pool modelling, Thermal stratification, Thermal fatigue, Above structure, Vessel cooling, Chemistry control and cover gas cooling, In-vessel fuel storage, Sloshing, Jet-stratification interaction or Jet mixing, Gas entrainment, Corium

cooling, steam generator tube rupture, integral research); and Reactor System Thermal Hydraulics (1-D codes or System codes improvement, Heat exchangers, Start-up heating system, Natural circulation stability, Multiscale thermal hydraulics, Thermal hydraulics coupled to neutronics, Liquid metal-water and -air interaction, Containment thermal hydraulics).

Reactor neutronics challenges are related to reactivity control in the reactor core, confinement of radioactivity, and handling of issues relating to the formation of toxic radioactive Po-210 with respect to lead liquid metal. In addition to the research activities aiming at designing neutron absorbing control rods and other regulators to control the thermal/fast fission process or neutron population/density in the reactor core, there is the need for research into understanding of the behavior and transport of fission products from the fuel pins, through the liquid metal coolant and cover gas region, into the containment dome, and finally into the environs.

In addition to research activities into thermal-hydraulics and reactor core neutronics, there is the need to look at the research activities that focus on the events that initiate accidents leading to the initial destruction of the core to severe destruction of the core and hence nuclear accidents. The reactor core is normally built to have inherent safety features to overcome mild accident initiating events but hypothetical accident initiating events such as anticipated events, unlikely events, severe unlikely and beyond design basis events should be researched into by various accident simulation techniques. Accidental scenarios including Unprotected Loss of Flow (ULOF), Unprotected Transient Overpower (UTOP), and Unprotected Loss of Heat Sink (ULOHS) with no or only minor fuel damage should be thoroughly investigated. Accident scenarios including transient overpower without scram (TOP WS); loss of flow without scram (LOF WS); overcooling accident without scram (OVC WS); loss of heat sink without scram (LOHS WS); loss of coolant accident without scram (LOCA WS) should also be investigated. The results of these studies help the designers to design reactors (1) to reduce the probability of a major accident to as low a level as practical [prevention] and (2) to provide features to mitigate the effects of core destructive accidents CDAs [mitigation].

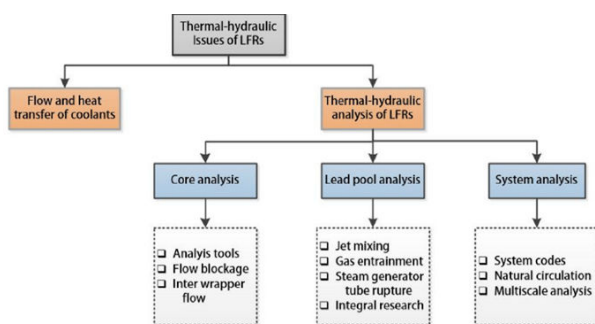


Figure 17: Outline of thermal-hydraulic issues of LFRs. (Zhang et al., 2019)

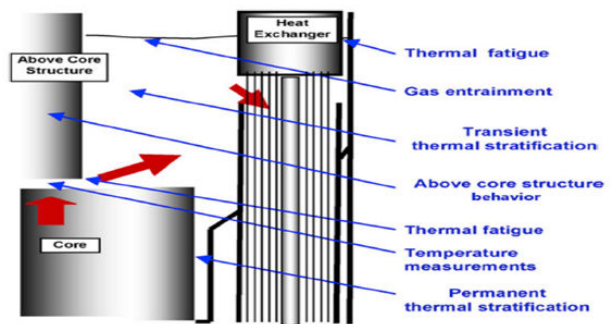


Figure 18: Thermal-hydraulic issues existing in the lead pool

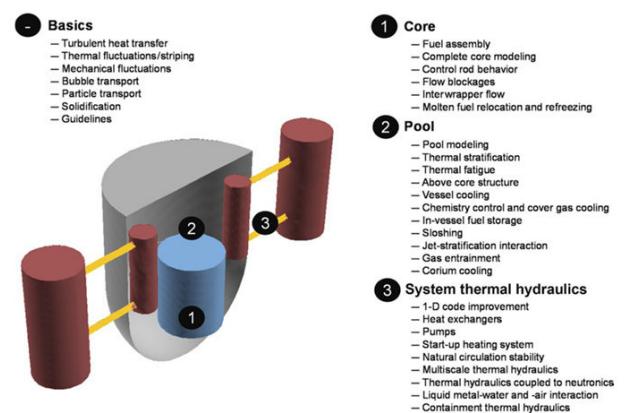


Figure 19: Overview of thermal-hydraulic challenges in liquid-metal-cooled reactors (Roelofs et al., 2019)

Some specific research concerns of LMFRRs are briefly discussed below

Various studies related to effects of mixing of fluid flows at different temperatures are needed to better understand the thermal fatigue phenomenon. Shorter lifespan of the components (Ageing) and structural integrity concerns could arise as a result of mixing effects of fluid flows which include Thermal fatigue, thermal stripping, thermal stratification, turbulent mixing, creep, corrosion and oxidation among others.

Research into the challenges arising from the usage of liquid metal coolants in the design and operation of LMFRRs. These challenges include chemical toxicity of lead vapors, oxidizing nature of corrosive molten lead for uncontrolled oxygen concentration and potential for lead to solidify because of its high melting/freezing point of 328°C; high probability of sodium leaking and reacting with air (easily burn in air) and water (easily explode in contact with water); handling of highly radiotoxic polonium produced during irradiation of lead-bismuth eutectic; and reactivity control among others.

More studies into liquid metal coolant interaction with water should SGTR occur during the process of heat transfer from the metal coolants to water for steam generation.

More studies also needed to understand issues relating to the liquid metal coolant interaction with the fuel rod in the reactor core.

Kim et al. provided several physical phenomena associated with core destructive accident (CDA) in various phases which include Initiating and Transition phases of nuclear accident, core material

movement and mild discharge, and energetic disassembly. These physical phenomena require future research and development efforts to better understand these phenomena which will guide the design of nuclear fuels and hence the design of reactor cores. Table 15 shows the list of these physical phenomena.

Table 15: Key Research and Development (R&D) items for the CDA Analysis

Phase of CDA	Key R&D items
Initiating phase	Axial fuel expansion; Clad material melting, movement, and freezing; Early fuel dispersal in sodium voided fuel elements; Fuel pin failure, failure propagation, and fuel movement in partly voided fuel elements
Transition phase	Fuel/steel penetration into axial and radial structures (blockage formation, remelting) Melt-through or mechanical failure of wrapper walls.
Phase of core material movement and mild discharge	Transient behavior of boiling fuel/steel pools Secondary excursions (space dependent kinetics) Steel vapor driven discharge of core material (contact with sodium)
Phase of energetic disassembly	Core material expansion and discharge in the presence of Sodium Behavior of upper core structures during energetic discharge of core material

Studies related to the estimation of radioactivity release and the corresponding potential exposure to the public with respect to the LMFRs should be carried out to understand various issues on public exposure to radiation as a result of accidental radioactivity release. These studies should take into consideration the source term, containment performance, radioactivity transport and release, and atmospheric dispersal. In addition to the research activities aiming at designing neutron absorbing control rods and other regulators to control the fast fission process or neutron population/density in the reactor core, there is the need for research into understanding of the behavior and transport of fission products from the fuel pins, through the liquid metal coolant and cover gas region, into the containment dome, and finally into the environs.

Comparison of the estimation of the total reactivity associated with the operations of the three liquid metals (Na, Pb and LBE) fast reactors. The total reactivity includes external reactivity, Doppler effects and expansion effects (or reactivity coefficients) in fuel, clad and coolant. The total reactivity estimation should also take into consideration void and density reactivity coefficients estimations.

Experimental and numerical studies required for generation mechanism, propagation processes and influence on reactor structures of pressure waves, and sloshing of the primary coolant pool (investigate the hydrodynamic forces and coupling effects between primary coolant and reactor structures).

Future experimental studies on local blockages in LBE-cooled rod bundles with wires spacers should focus on porous blockages, which are more likely to appear in a reactor.

Further studies of metal fuel relocation with pressure injection is necessary to find the effect of pressure on fuel fragmentation, relocation behavior in the core region. Understanding the relocation behavior of metallic fuel in severe accident scenarios is one of the most important factors in the safety assessment of sodium-cooled fast reactors (SFRs).

New experiment involving optical measurements of sodium vapor concentration is needed in order to extend the modeling capabilities towards prediction of sodium water reaction (SWR) effects including prediction of the quantity of sodium reacting at once during runaways and pressure effects.

Conclusions

Electricity generation from nuclear sources in the world is mostly from water-cooled NPPs. Efforts are being made to generate electricity from liquid metal cooled NPPs as well because of competitive advantages compared to water-cooled NPPs, and these efforts include various studies ranging from liquid metal cooled NPP concepts, design and operation. This work carried out brief review of studies done to support the design and operation of liquid metal cooled NPPs for electricity generation. This review covers lead, sodium and lead-bismuth-eutectic cooled NPPs of which lead and sodium cooled NPPs are among the GEN-IV NPPs being designed for operation in the near future. The review also covers recent experimental and computational studies as well provided some research concerns of liquid metal cooled NPPs that need attention to further contribute to the efforts being made to design and operate liquid metal cooled NPPs for electricity generation. The main findings from these studies include:

Various studies/researches into liquid metal (LM)-water interaction are found to be important and more data needed to understand issues concerning LM-water interactions. Pool type NPP designs of lead and lead-bismuth have heat exchange between the LM pool and water loop (secondary loop) occurring in the reactor vessel whereas the pool and loop type NPP designs of sodium have heat exchange between the LM loop and water loop occurring outside the reactor vessel. There is likelihood of SGTR occurring in the reactor vessel or outside the reactor vessel during the operation of LM cooled NPPs.

There is less data on lead cooled NPP designs available in literature compared to that of sodium cooled NPP designs.

There is less data on hypothetical accident initiating events to help understand and manage accident situations should in case they occur during the operation of LM-cooled NPPs. These hypothetical accident initiating events include anticipated events, unlikely events, severe unlikely and beyond design basis events.

There is less thermal hydraulics data on interaction of the fuel rod with LM-coolant.

There is less or no information on the probability safety analysis (PSA) of LM-cooled fast NPPs.

There is less data available in literature on sodium-water or sodium-air interaction because of the safety concerns of these types of experimentation, sodium easily burns in air and explodes in contact with water.

Studies on effects of fluid mixing in the reactor core to enhance fluid flow and heat transfer, and in the other T-Junction related parts of NPPs are found to be important and need more attention to help us understand effects such as thermal fatigue, thermal stripping, thermal stratification, creep, corrosion and oxidation. These effects can be induced by temperature and pressure fluctuations. These types of studies on fluid mixing effects which are related to LM-cooled NPPs when performed can be compared with similar studies relating to water-cooled NPPs.

Selection of turbulence models and the corresponding wall treatment models based on Yplus (y+) value for modelling fluid flow and heat transfer systems is found to be challenging task and if not handled well could affect the accuracy of the computational predictions.

To conclude, this brief review would be helpful to researchers as well as students and will also contribute to efforts being made to make design and operation of LM-cooled NPPs safer for electricity generation.

References

1. Addad, Y., Lee, J.I. LES and URANS predictions of thermal load in piping systems; T-Junction. International Conference on Nuclear Engineering, Proceedings, I CONE.2012;4(1):599–606.
2. Alfonsi, G. Reynolds-averaged Navier-Stokes equations for turbulence modeling. *Applied Mechanics Reviews*.2009; 62 (4): 1–20. ANSYS CFX-5.7.1. Turbulence and Near-Wall Modelling. 2005; 1-22.
3. ANSYS. Introduction to FLUENT Training, Turbulent Flows. 2006; 1-49.
4. ANSYS, Introduction to ANSYS FLUENT, Turbulence Modeling. 2010; 1-59.
5. ANSYS, 2015. Introduction to ANSYS CFX, Turbulence, pages. 2015; 1-42.
6. Arostegui, D.A., Holt, M. Advanced Nuclear Reactors: Technology Overview and Current Issues. Congressional Research Service, R45706. 2019; 1-47.
7. Arthur, E.M., Zhang, C., Debrah, S.K., Yamoah, S., Wang, L. Analysis of the drop dynamics of control rod assembly in a LBE-cooled research reactor, *Annals of Nuclear Energy*.2020; 149 : 107778.
8. Ayhan, H., & Sökmen, C. N. CFD Modeling of Thermal Mixing In T-junction: Effect of Branch Pipe Diameter Ratio. The 15th International Topical Meeting on Nuclear Reactor Thermal - Hydraulics, NURETH-15, paper number.2013;313.
9. Cao, L., Yang, G., Chen, H. Transient sub-channel code development for lead-cooled fast reactor using the second-order upwind scheme; *Progress in Nuclear Energy*.2019; 110:199–212.
10. Cd-Adapco. User Guide, STAR-CCM+ Version. 2015.
11. Cheng, L.-Y., Todosow, M., and Diamond, D., 2018. Phenomena Important in Liquid Metal Reactor Simulations. Technical Document, BNL-207816-2018-INR. 2018; 1-60.
12. Ciampichetti, A., Pellini, D., Agostini, P., Benamati, G., Forgiione, N., Oriolo, F. Experimental and computational investigation of LBE–water interaction in LIFUS 5 facility. *Nucl. Eng. Des.*209; 239: 2468–2478.
13. Courtin, S. High Cycle Thermal Fatigue damage prediction in mixing zones of nuclear power plants: Engineering issues illustrated on the FATHER case. *Procedia Engineering*. 2013; 66:240–249.
14. Dai, Y., Zheng, X., Ding, P. Review on sodium corrosion evolution of nuclear-grade 316 stainless steel for sodium-cooled fast reactor applications. *Nuclear Engineering and Technology* xx, xxx.2021.
15. David, L., Beauchamp, F., Allou, A., Daudin, K., Saurel, R. A small scale experiment and a simplified model to investigate the runaway of sodium-water reaction; *International Journal of Heat and Mass Transfer*.2019. 144: 118542.
16. Eggerston, E.C., Kapulla, R., Fokken, J., Prasser, H.M. Turbulent mixing and its effects on thermal fatigue in nuclear reactors, *World Acad. Sci, Eng. Technol.*2011. 76: 206–213.
17. Ferede, N. A. Numerical analysis and CFD simulation of fluid flow in T- Junction pipe By using ANSYS CFX. *International Journal of Scientific & Engineering Research*.2019.10 (10):1-11.
18. Hannink, M.H. C., Kuczaj, A.K., Blom, F.J., Church, J.M., & Komen, E M.J. A coupled CFD-FEM strategy to predict thermal fatigue in mixing tees of nuclear reactors. Proc. of EUROSAFE Forum, Paris, France. 2008.
19. Johnson, M., Journeau, C., Matsuba, K-i., Emura, Y., Kamiyama, K. Characterization of high-temperature nuclear fuel-coolant interactions through X-ray visualization and image processing. *Annals of Nuclear Energy*.2021; 151:107881.
20. Jeltsov, M. Validation and Application of CFD to Safety-Related Phenomena in Lead-Cooled Fast Reactors. Doctoral Thesis KTH Royal Institute of Technology, School of Engineering Sciences, Department of Physics, Division of Nuclear Engineering, SE - 106 91 Stockholm, SWEDEN. 2018; 11.
21. Jeltsov, M., Villanueva, W., Kudinov, P. Seismic sloshing effects in lead-cooled fast reactors, *Nuclear Engineering and Design*. 2018; 332:99–110.
22. Jeong, Y.S., Kim, J.Y., Bang, I.C. Enhanced heat transfer and reduced pressure loss with U-pattern of helical wire spacer arrangement for liquid metal cooled-fast reactor fuel assembly. *Annals of Nuclear Energy*.2020; 135 :106971.
23. Jeong, J-H., Song, M-S. CFD investigation of a JAEA 7-pin fuel assembly experiment with local blockage for SFR, *Nuclear Engineering and Technology* xxx, xxx.2021.
24. Kadak, A.C. A Comparison of Advanced Nuclear Technologies. The Center on Global Energy Policy, COLUMBIA SIPA. 2017; 1-112.
25. Kim, Y.C., Na, B.C., Hahn, D.H., 1997. Review of Core Disruptive Accident Analysis for Liquid-Metal Cooled Fast Reactors, KAERI/AR-463/97. 1997.
26. Kim, T., Harbaruk, D., Lisowski, D., Bremer, N., Farmer, M., Grandy, C., Chang., Y-II. Experimental studies on metallic fuel relocation in a pin bundle core structure of a sodium-cooled fast reactor. *Nuclear Engineering and Design*.2020; 365:110719.
27. Li, C.-J., Tsai, Y.-L., Tsai, T.-P., & Wang, L.-H., 2010. Two different turbulence models in comparison with experiments on thermal mixing phenomenon in a tee piping. *WSEAS TRANSACTIONS on FLUID MECHANICS*.2010;5(2):45–54.
28. Liang, Y., Chen, Y., Zhang, D., Liu, X., Deng, J., Wang, C., Tian, W., Qiu, S., Su, G.H. Experimental and numerical investigation on flow characteristics of inter-wrapper channel in LMFBR. *Annals of Nuclear Energy*.2021; 151: 107918.

29. Li, S.Z., Cao, L.K., Khan, M.S., Chen, H.L. Development of a sub-channel thermal hydraulic analysis code and its application to lead cooled fast reactor. *Appl Therm Eng.* 2017; 117: 443–51.
30. Liu, X.J., Yang, D.M., Yang, Y., Chai, X., Xiong, J.B., Zhang, T.F., Cheng, X. Computational fluid dynamics and subchannel analysis of lead–bismuth eutectic-cooled fuel assembly under various blockage conditions. *Applied Thermal Engineering.* 2019; 1-35.
31. Lyu, K., Chen L, Chen, L., Yue, C, Gao, S., Zhou, T., Huang, Q. Preliminary thermal-hydraulic sub-channel analysis of 61 wire-wrapped bundle cooled by lead bismuth eutectic. *Annals of Nuclear Energy.* 2016; 92: 243-250.
32. Matsuba, K.I., Isozaki, M., Kamiyama, K., Tobita, Y. Distance for fragmentation of a simulated molten-core material discharged into a sodium pool. *Journal of Nuclear Science and Technology.* 2016; 53 (5): 707–712.
33. Naik-Nimbalkar, V. S., Patwardhan, A. W., Banerjee, I., Padmakumar, G., & Vaidyanathan, G. Thermal mixing in T-junctions. *Chemical Engineering Science.* 2010; 65(22): 5901–5911.
34. Nakamura, H., Sibamoto, Y., Anoda, Y., Kukita, Y., Mishima, K., Hibiki, T. Visualization of simulated molten-fuel behavior in a pressure vessel lower head using high frame-rate neutron radiography. *Nucl. Technol.* 1999; 125: 213–224.
35. OTA -E-575. Aging nuclear power plants managing plant life and Decommissioning. United States Congress, Office of Technology Assessment (Washington, DC: U.S. Government Printing Office). 1993; 1-182.
36. Pacio, J., Daubner, M., Fellmoser, F., Litfin, K., Wetzel, T. Heat transfer experiment in a partially (internally) blocked 19-rod bundle with wire spacers cooled by LBE. *Nucl Eng Des.* 2018; 330: 225–40.
37. Perez-Valseca, A.-D., Quezada-García, S., Gomez-Torres, A.-M., Vazquez-Rodríguez, A., Espinosa-Paredes, G., 2019. Reactor behavior comparisons for two liquid metal-cooled fast reactors during an event of loss of coolant. *Case Studies in Thermal Engineering.* 2019; 16: 100556.
38. Pesetti, A., Del Nevo, A., Forgiione, N. Experimental investigation and SIMMER-III code modelling of LBE–water interaction in LIFUS5/Mod2 facility. *Nucl. Eng. Des.* 2015; 290: 119–126.
39. Roelofs, F., 2018. Introduction to liquid metal cooled reactors, Technical Document. 2018; 1-15.
40. Roelofs, F., Gerschenfeld, A., Tarantino, M., Tichelen, K.V., Pointer, W.D., 2019. Thermal-hydraulic challenges in liquid-metal-cooled reactors. Technical Document, pages 1-43.
41. Roelofs, F. Liquid metal thermal hydraulics: State-of-the-art and future perspectives. *Nuclear Engineering and Design.* 2020; 362: 110590.
42. Schriener, T.M., El-Genk, M.S. Comparative CFD analyses of liquid metal cooled reactor for lunar surface power. *Nuclear Engineering and Design.* 2014; 280: 105–121.
43. Sobolev, V. Database of thermophysical properties of liquid metal coolants for GEN-IV. Scientific Report of the Belgian Nuclear Research Centre, SCK•CEN-BLG-1069. 2010; 1-175.
44. Shitsi, E. Heat Transfer and Flow Instability Analysis on Parallel Channels with Water at Supercritical Pressure using STAR-CCM + CFD code. PhD thesis, Graduate School, University of Ghana, Legon. 2017; 1-184.
45. Sibamoto, Y., Visualization and measurement of subcooled water jet injection into high-temperature melt by using high-frame-rate neutron radiography. *Nucl. Technol.* 2002; 139: 205–220.
46. Sibamoto, Y., Kukita, Y., Nakamura, H. Small-scale Experiment on Subcooled Water Jet Injection into Molten Alloy by Using Fluid Temperature-Phase Coupled Measurement and Visualization. *Journal of Nuclear Science And Technology.* 2007; 44 (8): 1059–1069.
47. Štigler, J. Mathematical Model of the Unsteady Fluid Flow Through Tee-Junction. *Scientific Bulletin of the “Politehnica” University of Timisoara Transactions on Mechanics Tom Fascicola* 6. 2007; 52(66): 83-92.
48. Štigler, J., Klas, R., Kotek, M., Kopecký, V. The Fluid Flow in the T-Junction. The Comparison of the Numerical Modeling and Piv Measurement. XIIIth International Scientific and Engineering Conference “HERVICON-2011”, *Procedia Engineering.* 2012. 39: 19-27.
49. Štigler, J., Klas, R., & Šperka, O. Characteristics of the T-junction with the equal diameters of all branches for the variable angle of the adjacent branch. *EPJ Web of Conferences.* 2014; 67, 02110: 1-12.
50. Sutalo, F. Evaluation of Variants of Enhanced Wall Treatment Wall Function in Turbulent Flow Simulations. Master’s Thesis, University of Zagreb, Faculty of Mechanical Engineering and Naval Architecture. 2017; 1-127.
51. Tenchine, D. Some thermal hydraulic challenges in sodium cooled fast reactors. *Nucl Eng Des.* 2010; 240: 1195–217.
52. Tunstall, R., Laurence, D., Prosser, R., Skillen, A. Large eddy simulation of a T-Junction with upstream elbow The role of Dean vortices in thermal fatigue. *Applied Thermal Engineering.* 2016; 107: 672–680.
53. Visser, D.C., Roelofs, F., Mirelli, F., Tichelen, K.V. Validation of CFD analyses against pool experiments ESCAPE, *Nuclear Engineering and Design.* 2020; 369: 110864.
54. Wang, G. A review of research progress in heat exchanger tube rupture accident of heavy liquid metal cooled reactors, *Annals of Nuclear Energy.* 2017; 109 : 1–8.
55. Wu, Z., Lu, C., Morgan, S., Leon, S.B., Bucknor, M. A status review on the thermal stratification modeling methods for Sodium-cooled Fast Reactors. *Progress in Nuclear Energy.* 2020. 125, 103369.
56. Zhang, Y., Wang, C., Lan, Z., Wei, S., Chen, R., Tian, W., Su, G. Review of Thermal-Hydraulic Issues and Studies of Lead-based fast reactors. *Renewable and Sustainable Energy Reviews* xxx, xxx. 2019.
- 57.